Role of Glucose Transporters in osteoblastic cells

Master's Thesis

MSc Degree Programme in Biomedical Sciences

Drug Discovery and Development

University of Turku

November 2021

Sana Rais

sarais@utu.fi

Kaisa Ivaska-Papaioannou, Adjunct Professor

Institute of Biomedicine

University of Turku

Milja Arponen, MSc,

Institute of Biomedicine

University of Turku

The originality of this thesis has been verified in accordance with the University of Turku quality assurance system using the Turnitin Originality Check service.

UNIVERSITY OF TURKU
Institute of Biomedicine, Faculty of Medicine

Sana Rais; Role of glucose transporters in osteoblastic cell
Master's Thesis Project, 50 pages, 1 appendix
MSc Degree Program in Biomedical Sciences/Drug Discovery and Development
January 2022

ABSTRACT

Human skeleton is undergoing a constant remodeling through coupled actions of bone resorbing osteoclasts and bone forming osteoblasts and this remodeling process requires a constant source of energy for the cells. Different energy substrates such as glucose or fatty acids are thought to be important for osteoblastic differentiation and act as a fuel source for bones. Glucose is a major source of energy for cells, and it is transported into the cells via glucose transporter proteins (GLUTs).

To date, it is unclear which GLUTs are essential for osteoblasts. Therefore, this study aims to optimize silencing of GLUTs using siRNA technology to find out which of the known class I GLUTs are most important for the osteoblasts and to determine how energy is utilized by the osteoblasts and their precursors, the bone marrow stromal cells (BMSCs).

Three main class I GLUTs (GLUT-1, GLUT-3, GLUT-4) were detected at mRNA level in rat osteosarcoma cell line UMR-106 by quantitative polymerase chain reaction (qPCR) and at proteins level by immunofluorescence. We silenced each of these GLUTs individually by siRNA in the cell line and observed an efficient silencing (>90%) for each of the GLUTs. Our results demonstrates that siRNA constructs work efficiently in GLUTs silencing. Similar silencing was also observed in primary osteoblasts differentiated from rat BMSCs. We have also optimized primers for GLUT-5-10 and -12 and checked their expression in control tissues with qPCR.

In summary, we have established siRNA methodology for silencing of GLUTs in UMR-106 cell line and in BMSCs. These methods allow us to study the role of each GLUT in skeletal glucose utilization and we can further gain knowledge about the specific roles of each GLUT in osteoblast homeostasis and energy metabolism.

Keywords: bone, osteoblasts, GLUTs, siRNA, qPCR

Table of Content

1. Introduction

Skeleton is made up of bones and is essential for various functions such as locomotion, protection, and mineral homeostasis. To maintain the skeletal integrity, the equilibrium between the formation and resorption of the bone needs to be balanced. Adult skeleton is constantly remodelled, and an appropriate control of osteoblasts and osteoclasts is essential. Osteoblasts are responsible for bone formation while osteoclasts function in bone resorption. Therefore, bone cells need an efficient energy supply for constant remodelling. The understanding of bioenergetics of bone cells holds huge potential for the therapy of various bone diseases such as diabetes related bone diseases, osteoporosis or even osteosarcoma. In this study, our major focus is on the glucose as an energy source and the role of glucose carriers i.e., glucose transporters in osteoblast bioenergetics.

1.1 Bone and bone cells

Bone is a complex structure of connective tissues that consist of cells and an extracellular matrix that is mineralized simultaneously along with other tissues. It is composed of organic matrix and mineral phase called hydroxyapatite ($Ca_{10}(PO_4)_6(OH)_2$) while other minerals include magnesium, and carbonate. (Boskey, 2007). The hydroxyapatite crystals in bone are small in size, helping them to maintain mineral metabolism. Bone mineral substance facilitates the weight bearing strength and mechanical rigidity while the flexibility and elasticity of bone are maintained by the organic matrix (Katsimbri, 2017). Bone extracellular matrix contains the proteins with a particular function and structural proteins. Most of the matrix consists of collagen, primarily type I, but other proteins, known as non-collagenous proteins (NCP), are reported to weigh as much as 5% of the total weight of the bone. Collagen type I is the most abundant protein in the bone matrix and consists of three proteins chains which coil around each other forming a triple-helical molecule, in each of the chains (two alpha 1 chains and one alpha 2 chain) every third amino acid is glycine (Boskey, 2013). Bone also contains large amounts of water, attaching to crystals of mineral and cooperating with collagen fibrils (Yoder et al., 2011). Functional proteins control collagen fibril diameter, serve as growth factor, or signalling molecules, act as enzymes or exhibits further roles. With age, the concentration of these components in the body alters (Boskey and Coleman, 2010). The bone marrow cavity consists of bone marrow fat and composition of bone marrow fat cells is distinctive as they have unique properties compared to white adipocytes, such as gene expression,

composition of lipids, peripheral and local regulation. For bone function and bone marrow fat to correlate, there must be a balance between the amount and quality of adipose cells (Pino et al., 2016).

The three key cell types that exhibit the bone are bone cells; the osteocytes, bone forming osteoblasts and bone resorbing osteoclasts which are giant multinucleated cells emerging from the monocyte-macrophage line and dedicated to resorbing bone (Fattore, 2012). Bone forming osteoblasts and osteocytes originates from the mesenchymal stromal cells (MSCs) and they form the osteoblast lineage. The bone modeling is the process that changes the bone shape throughout growth and bone remodeling is the process that keeps the adult skeleton intact (Bellido et al., 2014). In the bone, osteocytes constitute 90–95% of the total number of cells and can live up to 25 years (Franz-Odendaal et al., 2005). The osteocytes get trapped during the bone-building process, and they are widely distributed inside the mineralized bone matrix. The osteoclasts and osteoblasts are regulated by osteocytes in response to mechanical and hormonal stimuli (Bellido et al., 2014).

1.1.1. Osteoblasts

Osteoblasts are the tissue-forming cells and in the bone, osteoblasts account for 4-6% of overall resident cells (Capulli et al., 2014). By synthesizing and secreting the bone matrix, they facilitate the mineralization of bone to keep calcium and phosphates in a balanced equilibrium. Osteoblasts originates from the MSCs which can differentiate into other cell types such as adipocytes, fibroblasts, myoblasts, and chondrocytes (Figure 1). Osteoblast cells morphology is diverse, often flat, round, cylindrical or cubic, with a 20 to 50 μm diameter. The osteoprogenitor cells differentiates into mature osteoblast. At their mature stage, they have alkaline cytoplasm, including many nucleosomes and abundant rough endoplasmic reticulum (Qiu et al., 2019). These cells display the morphology of cells that synthesize proteins, involving numerous Golgi apparatus, and rough endoplasmic reticulum along with several other secretory vesicles (Capulli et al., 2014; Marks and Popoff, 1988). A wide range of proteins are secreted by osteoblasts such as collagen, osteonectin, osteoponin, osteocalcin and in addition to being the earliest proteins secreted by osteoblasts. In addition, fibronectin also contributes to the formation of collagen fibrils (Velling et al., 2002).

Role of transcription factors Runx2 and Osx in osteoblast commitment

Transcription factors such as Runt-related transcription factor 2 (Runx2) and Osterix (Osx) are key regulators of MSCs differentiation and bone mineralization. Runx2 has a major role in the formation of bone, osteogenesis, by promoting maturation of chondrocytes and differentiation of osteoblasts during development of the skeleton. During initial stages of osteoblast development, Runx2 expression is dominant while in later stages of osteoblast differentiation Osx downstream factor for Runx2 is upregulated (Capulli et al., 2014). Runx2 transcription factor protein directly regulates fibroblast growth factor receptor 1-3 (Fgfr1-3) expression, osteoblast progenitors' proliferation, and fibroblast growth factor 2 (FGF2) induced proliferation via the FGF receptor (FGF-2/3) MAPK pathway. These findings suggest that for the proliferation and differentiation of osteoblast progenitor Runx2 is an essential transcriptional factor. Also, Runx2 controls proliferation primarily by enhancing Fgfr2 and Fgfr3 expression in osteoblast progenitors (Kawane et al., 2018). In osteoblasts and osteocytes, Osx is expressed, and it plays an essential role in differentiation and maturation of osteoblasts (Liu et al., 2020).

Expression of ALP and OCN during osteoblast differentiation

Alkaline phosphatase (ALP) is a glycoprotein that can exist in transmembrane or in a secreted form. The intestine, placenta, bone, liver, and kidneys are major sites of ALP expression in humans (Jo et al., 2018). ALP is considered as a biochemical marker of mineralization and can be used to monitor osteoblastic activity. ALP enzyme is used as a marker for bone formation and in vivo it functions as a catalyst for pyrophosphate conversion to monophosphate. Upon releasing these free monophosphate molecules, they enter the cell and facilitate formation of bone by triggering osteoblast differentiation (Figure 1) (Jo et al., 2018). Additionally, to increase ALP, osteoblastic activity must be increased since monophosphate can easily bind free calcium and forms calcium-phosphate complexes. The complexes contribute to osteogenesis and osteoblast differentiation from MSCs (Jo et al., 2018). During proliferation phase, ALP is produced by osteoblast progenitors and formation of pre-osteoblasts takes place. Pre-osteoblasts have high activity of ALP, and they secrete bone matrix proteins actively.

Whereas in mature osteoblasts, there is high expression of proteins such as osteocalcin (OCN) and collagen type I due to which they mineralized by embedding in bone matrix (Capulli et al., 2014). OCN

is one of the abundant proteins that is manufactured particularly by osteoblasts. OCN contains three γ-carboxyl glutamic acid residues which provides great affinity to hydroxyapatite in bone matrix (Zoch et al., 2016). Osteocalcin has different forms: carboxylated osteocalcin (cOC) and uncarboxylated osteocalcin (unOC) are both present in the circulation where the cOC type has higher affinity for calcium so it adheres to bone mineral but unOC type do not bind. For bone formation, OCN is commonly utilized as a serum marker for osteoporosis (Rubert and de la Piedra, 2020).

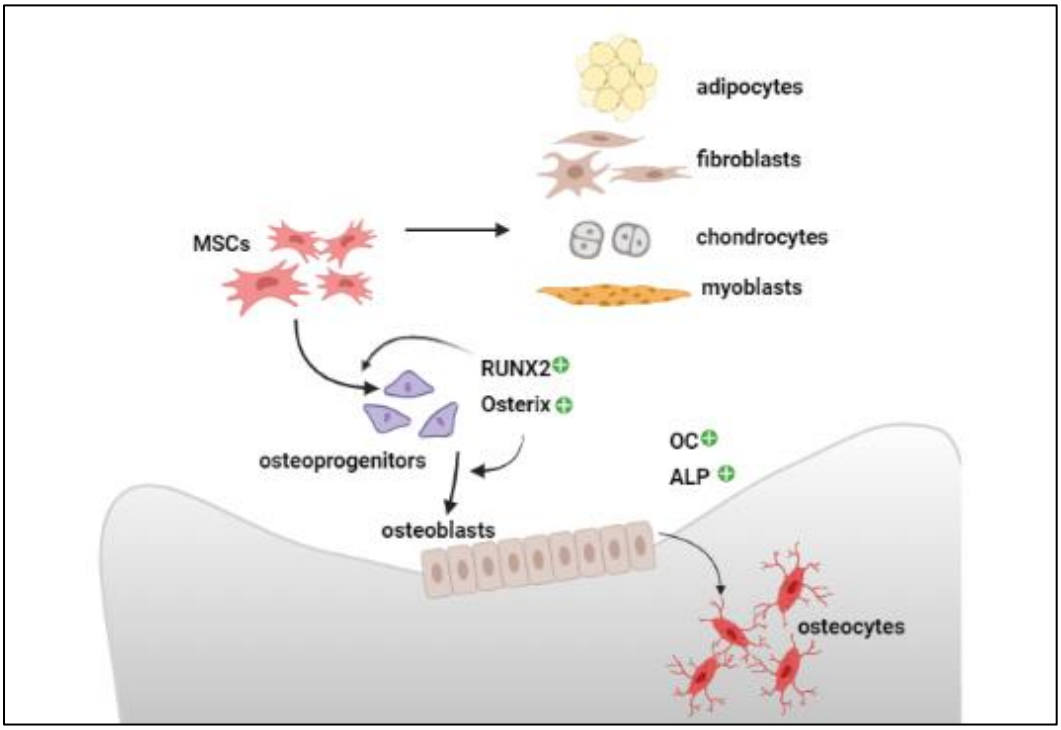

Figure 1: Formation of osteoblasts from mesenchymal stromal cells and the role of transcriptional factors and proteins (Created in BioRender.com)

1.1.2 Osteoclasts

The osteoclast is responsible for resorption of bone. The osteoclasts are large multinucleated cells that secretes hydrogen and chloride ions along with matrix metalloproteinases and cathepsin K at the site of bone resorption to break down bone tissue (Ono and Nakashima, 2018). Osteoclasts are differentiated from monocytes, macrophage lineage by activation of myeloid cells that express receptors c-Fms and Receptor activator of nuclear factor κ B (RANK), the necessary receptor for osteoclastogenesis. An understanding of the differentiation and activation of osteoclasts appears from the RANK ligands and

osteoprotegerin (OPG), which collectively regulate osteoclast differentiation (Soysa et al., 2012). The parathyroid hormone (PTH) induces osteoclast differentiation by activating expression of macrophage stimulating factor (MCSF) and RANK (Katsimbri, 2017). In addition, there are three steps in the differentiation of osteoclasts; first is the early differentiation when proliferation of hematopoietic stem cells (HSCs) occurs in the macrophage lineage, second it progresses into early osteoclasts precursors step along the expression of tartrate-resistant acid phosphatase (TRAP) and calcitonin receptor and third is when the fusion takes place (Soysa et al., 2012). During osteoclastogenesis, osteoclasts are differentiated for resorption, they polarize and create distinctive membrane regions such as the rough border, functional secretory area, and the sealing zone (Mulari et al., 2003).

1.1.3 Osteocytes

Osteocytes are generally defined as terminally differentiated osteoblasts, and they are located in small lacunae in mineralized bone. They are sensitive to mechanical stress, respond to pressure and tend to communicate with osteoblasts and osteoclasts via an intricate network of neural processes known as canaliculi (McGee-Lawrence et al., 2013). During the maturation of osteocyte, pre-osteocytes get embedded in the osteoid. The pre-osteocytes secrete factors that prevent mineralization locally and form cavities around the main body of bone cells (Bradshaw and Dennis, 2010). Osteocytes adapt to their microenvironment, send signals to the surface of bone for bone resorption or bone formation and control local and systemic mineral homeostasis. All these functions are accomplished through release of soluble factors and gap junctions with cells on bone surface (Bradshaw and Dennis, 2010). They can also modify molecules, synthesize new ones, and transmit signals through long distances (Nahian and AlEssa, 2021). The osteocytic proteins, such as sclerostin, contribute to metabolism of minerals which controls phosphate and biomineralization. Additionally, they work as endocrine regulators for metabolism of phosphates and regulate bone mass (Nahian and AlEssa, 2021). Osteocytes are thought to produce signals that reduce the rate of bone apposition of osteoblasts during replenishment of basic multicellular units (BMUs) and facilitate the conversion of osteoblasts into osteocytes (Kogianni and Noble, 2007).

1.1.4 Bone remodelling cycle

The bone maintains itself and restore by remodelling as this mechanism provides a process for an instant access to phosphate and calcium to regulate mineral homeostasis (Kenkre and Bassett, 2018). A series of events take place within BMU that consists of capillary blood vessels, osteoclasts, and osteoblasts. The composition and structure of BMUs depend on whether they are inside cortical or trabecular bone. In both locations, the BMUs consist of different cells that defines the bone remodeling compartment (BRC). BRC is the area for remodelling and is closely coupled with osteoclasts and osteoblasts. In cortical and trabecular bone, the remodeling cycle (Figure 2) takes place in a well-controlled and categorized manner with five corresponding phases: **activation, resorption, reversal, formation, and mineralization or termination** (Kenkre and Bassett, 2018).

Activation is the first and foremost step of bone remodelling where osteoclast precursors from circulation are recruited and activated. BMU is in dormant state before this step and bone detects the remodeling signal for the initiation (Katsimbri, 2017). Following the signal detection, bone lining cells retract, and collagenase digest the endosteal membrane. Then the differentiation of osteoclasts takes place, and the multinucleated large osteoclasts migrate to adhere on the bone surface thereby, initiating the resorption of bone by break down of matrix by secreting hydrogen ions and other proteolytic enzymes to resorption lacuna (Katsimbri, 2017).

Resorption in the remodeling cycle continues between 2-4 weeks. In the resorbing compartment, osteoclasts pump protons produced by Carbonic Anhydrase II to dissolve bone mineral. In particular, the H^+ -ATPase transports H^+ to spaces known as lacunae, which are linked with Cl^- transport via chloride channel hence preserving electroneutrality (Kenkre and Bassett, 2018). Additionally, degradation of the organic bone matrix occurs by the secretion of several enzymes such as cathepsin K and metalloproteinases. Howship's lacunae are spaces that forms on the surface of the trabecular bone because of this phenomenon and apoptosis of osteoclasts occurs at the end of resorption phase (Katsimbri, 2017).

Reversal phase takes place when bone resorption switches to formation in about four to five weeks. Several cells are recruited during reversal phase such as monocytes and pre-osteoblasts to begin formation of bone. The mononuclear cells are thought to mediate the bone formation (Katsimbri, 2017). In the preparation of the bone surface, cells from osteoblastic lineages secretes unmineralized collagen

matrix and accumulate to promote adherence of osteoblasts. Bone formation initiates as osteoblast-lineage cells replace osteoclasts (Kenkre and Bassett, 2018).

Formation of bone is also known as ossification or osteogenesis. During bone formation, osteoblasts are responsible for synthesizing the new proteinaceous matrix to fill up the spaces that are left by osteoclasts. The osteoid is the unmineralized bone matrix and is made up of collagen I and other proteins. Local growth factors influence the precursors of osteoblasts to proliferate and mature osteoblasts creates organic bone matrix at the resorbed area. As new bone matrix is mineralized the secretion of type I collagen occurs that forms collagenous matrix and alkaline phosphatase expression increases. They gradually decrease during the progression of matrix mineralization. Furthermore, when mineralization is concluded, osteoblasts can either differentiate into bone-lining cells and finally into osteocytes or undergo apoptosis and embedding themselves in the bone matrix (Katsimbri, 2017).

Termination is the last and final phase in the bone remodeling cycle during which mineralization of bone occurs that initiates in a month following the formation of osteoid (Jo et al., 2018). Consequently, as remodeling cycle ends the sclerostin expression gets activated and through the expression of this antagonist of Wnt signaling pathway osteocytes execute a critical function in signaling termination of bone remodeling (Kenkre and Bassett, 2018).

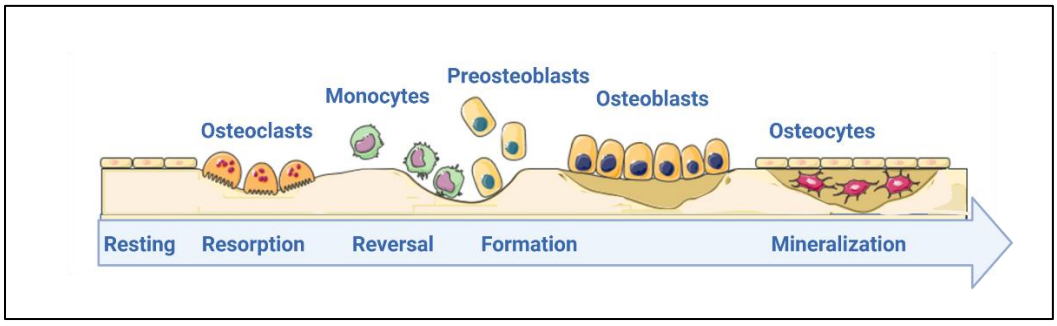

Figure 2: Bone remodeling cycle (Created by Servier Medical Art)

1.2 Glucose transporters

Glucose transporters (GLUTs) are proteins that transfer glucose and other hexoses through cell membrane. Currently in humans, there are 14 known members of the GLUT family, and they are

encrypted by genes in *SLC2A* family (Dwyer et al., 2002). These members of GLUT family are grouped into three classes according to their characteristics: Class I, Class II and Class III. The classification of GLUTs into subclasses is determined based on their similarity of amino acid sequences, for instance, class I facilitators are GLUT-1, -2, -3 and -4, class II facilitators are GLUT-5, -7, -9 and -11 and while class III facilitators are GLUT-6, -8, -10, -12 (Table 1). GLUT-13 is not similar to any of the other members, so it is separated to class IV (Joost and Thorens, 2001).

GLUT-1 is the highly expressed glucose transporter in brain and erythrocytes and appearing in only low amounts in fat, muscle, and liver. It is also the major GLUT during embryonic development and is considered to be responsible for low level glucose uptake in all cells. In addition to glucose uptake, they support translocation of aldoses, including pentose and hexose (McAllister et al., 2001; Mueckler and Makepeace, 2008).

GLUT-2 is primarily expressed in pancreas and liver where it functions as glucose transporter. In addition, it is also characterised as a high capacity and high affinity glucose sensor. In pancreas, by closing the K channel, glucose oxidation products such as ATP reduce K^+ efflux from the pancreatic β-cells and cause their membrane to depolarize. As a result, insulin is secreted in response to calcium influx (Jurcovicova, 2014). Additionally, GLUT-2 facilitates transepithelial glucose transport into the blood as in kidney basolateral membrane and in intestinal epithelial cells it is expressed (Barron et al., 2016).

GLUT-3 expression in human tissues in widely distributed though it is known as a neuro-specific GLUT as the expression of GLUT-3 is prevalent in the brain. The expression of GLUT-3 is also found in the testis, kidney, and the placenta. This transporter appears also to function in several tumors by facilitating glucose uptake with a high glucose requirement since it exhibits high affinity for glucose (Barron et al., 2016). In addition, this transporter is present both in dendrites and axons, and its expression correlates with cerebral utilization of glucose in different brain regions (Simmons, 2017).

GLUT-4 expressions are mainly found in adipocytes, muscles, and heart. In adipose and muscle tissues, glucose uptake occurs in response to stimulation of insulin which is essential for homeostasis of whole blood glucose. During basal conditions, less amount of glucose is taken up by the cells (Brewer et al., 2014). GLUT-4 levels increase with an increase in insulin levels as insulin activates the translocation of

GLUT-4 from intracellular areas towards plasma membrane (Li et al., 2016). Moreover, in type II diabetes mellitus (T2DM), due to impaired insulin-stimulated glucose transport the expression of GLUT-4 in skeletal muscles are reduced which shows the importance of GLUT-4 in the pathogenesis of T2DM and obesity (Thorens and Mueckler, 2010).

GLUT-5 is characterised by a strong fructose specificity. The apical membrane of intestinal epithelial cells is a primary site for the expression of this transporter, where it facilitates the absorption of dietary fructose. There are several other tissues in which it is present at lower levels, including muscle, brain, testes, fat, and kidney. Furthermore, the regulation of GLUT-5 occurs by several factors such as availability of substrate or diurnal rhythm. There is a correlation between an increase in fructose consumption and obesity, metabolic syndrome, and T2DM that has sparked research interest (Thorens and Mueckler, 2010).

GLUT-6 expressions are found in the leucocytes, brain and spleen but has also been shown to be upregulated in certain types of cancer, including endometrial cancer. Knockdown of GLUT-6 in endometrial cancer cells increases the susceptibility of cells to apoptosis (Caruana et al., 2019).

GLUT-7 is a facilitative glucose transporter that has a high affinity for fructose and glucose. It is closely related to GLUT-5. GLUT-7 expressions are found in the colon epithelia and small intestine apical membrane A minimal amount of its mRNA is identified in the prostrate and the testis (Li et al., 2004).

GLUT-8 expressions are found mainly in testis and brain while less expression is found in liver, spleen, kidney, and skeletal muscle. It is located intracellularly due to which it is thought that GLUT-8 might also be insulin-responsive (Augustin, 2010). It contains a motif of an amino acid that is not observed in either GLUT-4 or GLUT-1, that leads to an unknown late endosomal/lysosomal compartment. GLUT-8 expressive cells are thought to aid in efficient protein secretion. Due to the increased antibody production observed in activated β cells, this function is consistent with the upregulation of GLUT-8 observed in these cells (McBrayer et al., 2012).

GLUT-9 is a urate transporter detected in the intestine, liver, and kidney, as well as in relatively low levels in chondrocytes. Inactivating mutations of GLUT-9 cause hypouricemia, indicating that it is involved in urate reabsorption. This demonstrates its importance as a urate receptor by allowing urate to access its degrading enzyme uricase in the liver and to renal tubules where it may participate in urate

reabsorption. However, liver-specific loss of GLUT-9 gene function causes hyperuricemia, with no other physiological abnormalities, and elevated blood uric acid levels can result in atherosclerosis, insulin resistance and hypertension (Thorens and Mueckler, 2010).

GLUT-10 is composed of longer amino acid chains than other established members of the GLUT family, but almost identically protracted to GLUT-9 homologue (541 amino acids vs 540 amino acids) (Dawson et al., 2001). It has a sequence similarity of 31% to GLUT-1 33% to GLUT-8 and 35% to GLUT-6. GLUT-10 mRNA has been observed in pancreas, salivary gland, liver, adrenal, ovary, placenta, lung, thyroid, skin, and prostate (Dawson et al., 2001).

GLUT-11 is principally observed in slow-twitch fibres, where it is primarily linked with intracellular structures such as sarcolemma. In fast and slow twitch fibers, glucose transport is largely controlled through contraction and insulin (Gaster et al., 2004). GLUT-11 possesses three distinct forms that differ at the N-terminal end of proteins and are expressed in a variety of tissues (Thorens and Mueckler, 2010).

GLUT-12 is expressed in heart, skeletal muscle, prostate, and small intestine. In comparison with other GLUTs, the function and regulation of GLUT-12 is relatively little known. GLUT-12 expression was first detected in MCF-7 breast cancer cells (Augustin, 2010). Additionally, in various types of cancers GLUT-12 expression has been observed such as astrocytomas breast cancer, lung cancer, colorectal and prostate cancers, oligoastrocytomas and rhabdomyosarcomas (White et al., 2018).

GLUT-13 is not a glucose transporter but classified into GLUT family based on sequence similarity. It is a proton-coupled myoinositol transporter (HMIT) and this is one of the exclusive GLUT proteins which serves as a proton-coupled symporter and is expressed mainly in the brain (Thorens and Mueckler, 2010). Variants of GLUT-13 are thought to be related with mood disorders as it exhibits a myoinositol metabolism role in brain, which is linked with membrane trafficking at growth cones and at synapses (Williams et al., 2002).

GLUT-14 protein is categorized in class I and with GLUT-3 protein structure it shares a high degree of similarity, suggesting it as a glucose transporter (Thorens and Mueckler, 2010). There are twelve membrane-spanning helices on GLUT-14, and sugar transporter signature patterns have been shown previously to be crucial for sugar transport. Loop 1 contains the putative glycosylation site for GLUT-

14. There is a likelihood that GLUT-14 will be a hexose transporter, although substrate specificity, localization, and regulation may differ from those of GLUT-3 (Wu and Freeze, 2002).

Table 1: Isoforms of human Glucose Transporters

Classification of Glucose Transporters	Tissue location	Substrate and Affinity (Km)
Class I		
GLUT-1	Bone, brain, erythrocytes, Blood brain barrier, cell membranes	Glucose, 1-2 mM
GLUT-2	Liver, kidney, brain, islets of Langerhans, intestine	Glucose, 15-20 mM Glucosamine, 0.8 mM
GLUT-3	Neuron, placenta, testis	Glucose, 1-2 mM
GLUT-4	Skeletal muscle, adipose cells, heart	Glucose, 5mM
GLUT-14	Testis	Not known
Class II		
GLUT-5	Small intestine, brain, kidney	Fructose, 10-13 mM
GLUT-7	Small intestine, colon, testis, prostrate	Fructose, 0.3 mM
GLUT-9	Kidney, liver	Fructose, 0.42-0.09 mM
GLUT-11	Heart, liver, lung, brain, muscle	Fructose
Class III		
GLUT-6	Brain, spleen, leucocytes	Not known
GLUT-8	Testis, brain, liver, spleen, kidney, skeletal muscle	Glucose, 2 mM
GLUT-10	Heart, liver, pancreas	Glucose 0.3 mM
GLUT-12	Spleen, kidney, liver, lung, prostrate, skeletal muscle, placenta	Not known
GLUT-13	Brain	H+/myo-inositol co-transport

1.3 Energy utilization and glucose transporters in osteoblasts

It has long been known that glucose is a necessary nutrient for osteoblast cells; additional evidence indicates osteoblast-lineage cells express several GLUTs (Karner and Long, 2018). In osteoblast lineage,

GLUT-1 is highly expressed and has been demonstrated to be involved with Runx2 in a feed-forward mechanism that defines the bone formation extent during embryogenesis and during the course of life (Wei et al., 2015). In addition, GLUT-1 expression precedes the expression of Runx2 in osteoblasts, that can affect differentiation of osteoblast and formation of bone. When glucose enters the osteoblast via GLUT-1, activity of AMP-activated protein kinase (AMPK) is inhibited, resulting in increase in mammalian target of rapamycin complex 1 (mTORC1) activity. Secondly, glucose uptake inhibits the ability of AMPKs to promote ubiquitination of Runx2 in part through SMAD ubiquitination regulatory factor 1 (SMURF1). Because of these dual roles of AMPK in osteoblasts, agonists of AMPK activity have a detrimental effect on the formation of bone, see Figure 3 (Wei et al., 2015).

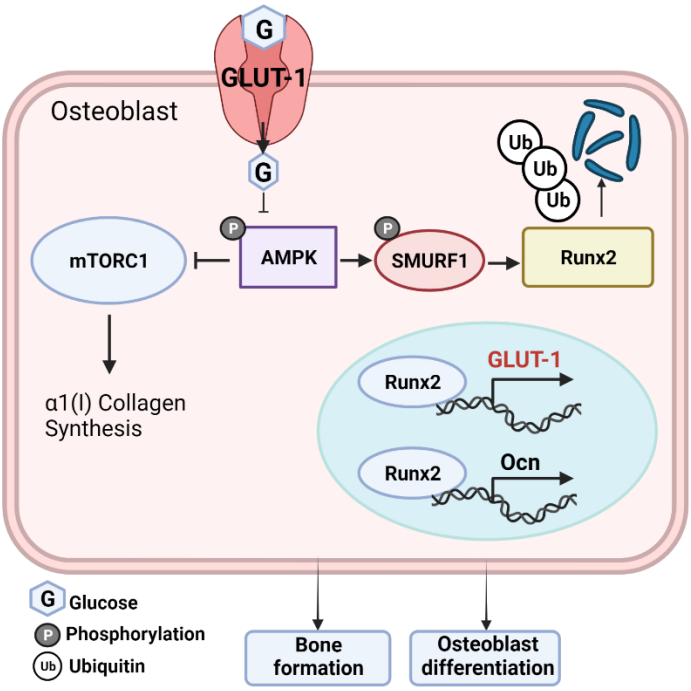

Figure 3: Graphical presentation of downstream effects of GLUT-1 in osteoblast (Modified from Wei et al., 2015 in BioRender.com)

Studies on the role of GLUT-1 in regulating Wnt7b anabolic function of bone in vivo and in vitro have found that the deletion of GLUT-1 in osteoblast lineage cells impairs osteoblast mineralization and differentiation in vitro. Consequently, these results provide evidence that glucose metabolism is important for Wnt7b-induced formation of bone and osteoblast differentiation (Chen et al., 2019).

In mature osteoblasts, GLUT-4 is maximally expressed concomitant with the maximal insulin-induced glucose uptake, indicating a crucial role for GLUT-4 in regulating energy needs for synthesis of matrix and mineralisation. Moreover, increased glucose uptake is associated with insulin-induced GLUT-4 translocation to the plasma membrane. When GLUT-4 is eliminated in the osteoblasts in vitro, glucose uptake is prevented by insulin-stimulation (Li et al., 2016). Recently, GLUT-6 protein expression was detected in bone marrow-derived macrophages (Caruana et al., 2019).

Other potential energy sources for osteoblasts includes glutamine, which is one of the most common amino acids in human plasma with the concentration of 500 to 750 μM. It has been observed that glutamine plays an important role in osteoblast metabolism, including glutamine active uptake and metabolism in explants of long bones and calvaria (Lee et al., 2017). The consumption of glutamine by BMSCs, which include precursors of osteoblast, decreases with ageing, and is associated with impaired osteoblast differentiation in mice (Huang et al., 2016). It has also been demonstrated that in precursors of osteoblasts, the oxidized glutamine promotes the production of energy in mitochondrial structures through its conversion to citrate (Karner et al., 2015). Additionally, glutamine-to-glutathione conversion contributes not only to the production of energy but also to redox homeostasis for implanted osteoblast precursors (Lee et al., 2017). Moreover, in addition to essential amino acids, non-essential amino acids also play an important role in osteoblast differentiation. In terms of mechanisms, the activating transcription factor 4 (ATF4) which is an osteoblastic transcriptional factor, increases uptake of amino acids and synthesis of collagen. Essential amino acids regulate the osteoblastic cells growth and differentiation and increase growth of the cells in a dose-dependent approach (Conconi et al., 2001).

Skeletal cells as well as bone marrow cells may consume fatty acids for energy requirements since adipocytes store fatty acids in the bone marrow for use in hematopoiesis and perhaps also bone remodeling (Pino et al., 2016). During ATP synthesis, degradation of fatty acids occurs in mitochondria after transfer from a carnitine-mediated transport pathway. Tri-acyglycerides are converted into fatty acids through lipolysis, where they are distributed into circulation (Lee et al., 2017). In addition, bone marrow fatty acids composition was found to be higher in saturated, and lower in unsaturated fatty acids in contrast to the free fatty acid pool in circulation (Pino et al., 2016). Additionally, in Krebs cycle (TCA), hydronated form of flavin adenine dinucleotide FADH2 and reduced nicotinamide adenine dinucleotide NADH are generated when pyruvate generated from glucose, is transported inside mitochondria via

mitochondrial pyruvate transporter (MPC) (Lee et al., 2017). In humans, the MPC gene encoding pyruvate transport has recently been identified and it has been observed that severe developmental defects are associated with impaired transport. When exogenous pyruvate is added to calvarial osteoblasts, oxygen consumption increases, signaling increased ATP production because of oxidative phosphorylation but recent studies also suggests that pyruvate levels increase osteoclastogenesis which shows that pyruvate plays role in bone formation and resorption (Lee et al., 2017).

Insulin is a potent stimulus for gene expression of OCN and osteoblast differentiation in the skeleton (Fulzele et al., 2010). Additionally, it influences the interaction of Runx2 and mice deficit of insulin receptors specifically in osteoblasts have a greater tendency to accumulate body fat and develop hyperglycemia due to hyperinsulinemia and inadequate insulin sensitivity. Moreover, in osteoblasts the insulin signaling takes place as osteoblast cells express the receptors for insulin. By regulating osteoblast function, insulin affects physiology and development of bone. Osteoblasts express the insulin receptors and interaction of osteoblasts with insulin enhances anabolic markers of bone such as ALP formation, uptake of glucose and synthesis of collagen (Fulzele et al., 2010).

1.4 RNAi

RNA interference (RNAi) technique has appeared as an effective tool in research studies for function of genes not only in human cells but also in animals. RNAi includes several approaches like short hairpin RNAs (shRNA) and short interfering RNA (siRNA) (Moore et al., 2010). The shRNA and siRNA methodologies utilize same mechanism of action in cells but the selection of method for both depends on numerous factors like type of the cells, time consumption and stable or transient binding requirements.

1.4.1 miRNA

MicroRNAs (miRNAs) are a class of around 22 nucleotides long, non-coding, single RNAs that function as posttranscriptional silencing molecules by binding to specific site of mRNA targets. They are biological and naturally expressed in cells while shRNA and siRNA are synthetic. The miRNA induces translational repression of the target gene or promote fast degradation of it, based on how well they complement their target mRNAs (Mallory and Vaucheret, 2006). In humans, about 3% of genes are miRNA-encoding, and 40-90% of protein-encoding genes code also a miRNA (Bentwich et al., 2005).

miRNAs are also obtained from introns that are within protein-coding genes or from specific miRNA genes (Tan et al., 2009). Multiple miRNAs have been implicated in osteoblast differentiation. These miRNAs may regulate vital transcription factors and developmental signaling molecules, as well as their receptors that are critical for the intricate osteogenesis and other biological processes (Hu et al., 2010). Many human diseases are associated to abnormal expression of miRNAs, where extracellular miRNAs can be studied as biomarkers of several diseases such as cancer, diabetes, cardiovascular and other diseases (O'Brien et al., 2018).

1.4.2 shRNA

The shRNA is comprised of two complementary synthetic RNA sequences that are 19-bp to 22-bp long and connected by a noncomplementary sequence of 4 to 11 nucleotides, creating a short loop comparable to that of the natural miRNA. Intracellularly, it is synthesized by creating vector-mediated DNA and they can be transfected as plasmid vectors by translating shRNAs which are transcribed by RNA polymerase III (Taxman et al., 2010). Lentiviral transfection of shRNA into osteoblasts in vitro is one of the strategies that has been used to study novel regulators for osteoblastic differentiation but there are many drawbacks related to lentiviral shRNA as it is not only costly, and time consuming but also high safety measurements are required (Ahmad et al., 2018).

1.4.3 siRNA

The siRNA carriers have achieved a remarkable momentum, thanks to their biochemical predictability and therapeutic potential. siRNAs were found in plants and later discovered in mammalian cells by endonucleolytic cleavage of the mRNAs they regulate (Tomari, 2005). In response to foreign nucleic acids such as virus, transposons, and transgenes the siRNAs defend the genome from alterations (Meister and Tuschl, 2004). siRNAs are 20-25 nucleotide long and they originate exogenously such as from the triggering of transgene, virus or transposon. The siRNA silencing feature is a pioneering method to downregulate expression of a target gene. As illustrated in Figure 4, siRNA is excised from double-stranded RNAs (dsRNAs) and works by pairing with complementary sequence in target mRNA and forming a complex with RNA-induced silencing complex (RISC). This mRNA-siRNA-RISC complex will initiate mRNA cleavage to small fragments due to which mRNA levels gets reduced in the cytosol

and this causes downregulation of the target gene expression and eventually downregulation of protein levels (Ghadakzadeh et al., 2016).

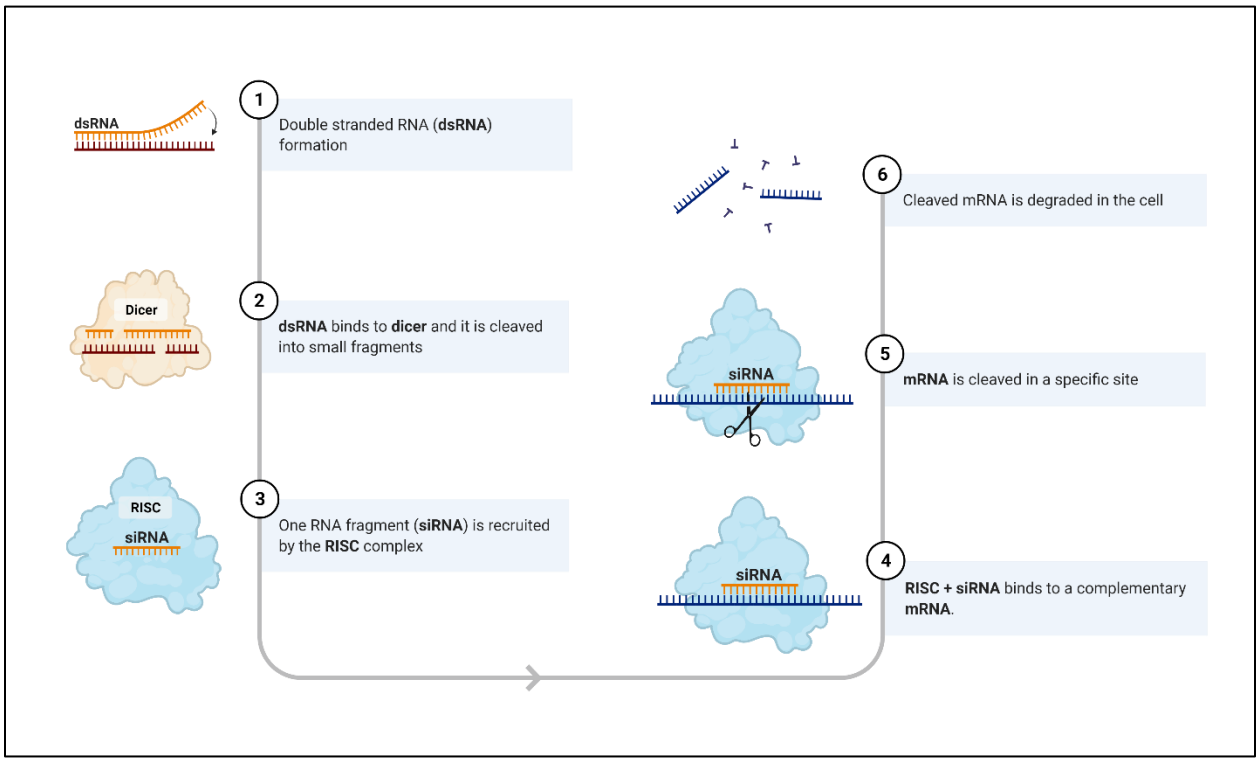

Figure 4: siRNA mechanism of action (Adapted from BioRender.com)

The siRNA is bounded and complexed into supramolecular assemblies appropriate for cell uptake with thermodynamic forces between cationic carriers and siRNA. In addition to stabilizing siRNA complexes and cell delivery, thermodynamic forces may determine siRNA efficacy in gene silencing (Aliabadi et al., 2012). Furthermore, siRNA stability in body fluids must also be considered to protect siRNA from oxidation and degradation (Aliabadi et al., 2012). The two main types of siRNA delivery systems are virus-based (viral vectors), such as lentiviral transfection of target cells, and non-viral vectors, such as liposomes. The advantage of non-viral vector delivery is when it comes to the formulation and industrial scale-up of peptides, polymers, and lipids (Pulford et al., 2010).

1.5 Hypothesis and Aims of the research

1.5.1 Hypothesis

At present, it is not known which and how many of GLUTs are expressed in osteoblasts and which ones of them are most important for osteoblast function. Existing data is conflicted since it is obtained with transformed cell lines and there is no information about silencing of GLUTs in normal osteoblastic cells i.e., non-cancerous cells. Previous experiments in the research group (unpublished) have collected data for the expression of GLUT-1, GLUT-2, GLUT-3, and GLUT-4 in primary rat bone marrow MSCs and osteoblasts during osteoblast differentiation and additionally, rat osteoblastic osteosarcoma cell line UMR-106. Preliminary data suggested that osteosarcoma cells and primary rat osteoblasts express GLUT-1, GLUT-3, and GLUT-4, but GLUT-2 expression was not found.

1.5.2 Aims

The major objective of this research is to find out how glucose is consumed by BMSCs during osteoblast differentiation by characterizing class I GLUTs and also to determine which one or ones of them are crucial for osteoblast survival and functions. In this project, each class I GLUT, GLUT-1, GLUT-3, and GLUT-4 was silenced individually by using siRNA technology. Later we will evaluate the effect of silencing on osteoblast function and bone formation. As a model for an osteoblast, we used bone marrow derived MSCs isolated from rat long bones and differentiated into osteoblasts *in vitro*. The transfection of siRNA constructs was first optimized using rat osteosarcoma cell line UMR-106 and then tested on primary cells. The specific aims of this project included are following:

1. To optimize siRNA-based silencing of GLUT-1, GLUT-3, and GLUT-4 in rat osteosarcoma cell line UMR-106 and then apply the optimized silencing method on primary rat osteoblasts.
2. To silence GLUTs either individually or combination with siRNA to determine which one of them are important for osteoblast function.
3. To screen if other members of glucose transporter family from GLUT-5 to GLUT-12 are present in UMR-106 cells and primary cells.

2. Results

2.1 siRNA transfection in UMR-106 and Primary Cells

Fluorescence-labeled siRNA was used to confirm transfection in both UMR-106 osteosarcoma and BMSCs. Figure 5 presents uptake of fluorescent siRNA, indicated by red colour (A) and (C) are EVOS microscopy of fluorescent-labeled transfection control siRNA. While (B) and (D) represents overlay images of Phase-Contrast and fluorescent-labeled transfection control siRNA.

Our results represent that 10 nM concentration of siRNA constructs A/B/C was optimum to get siRNA into the cells. A negative control was also used in our experiments which displayed no background signal (data not shown).

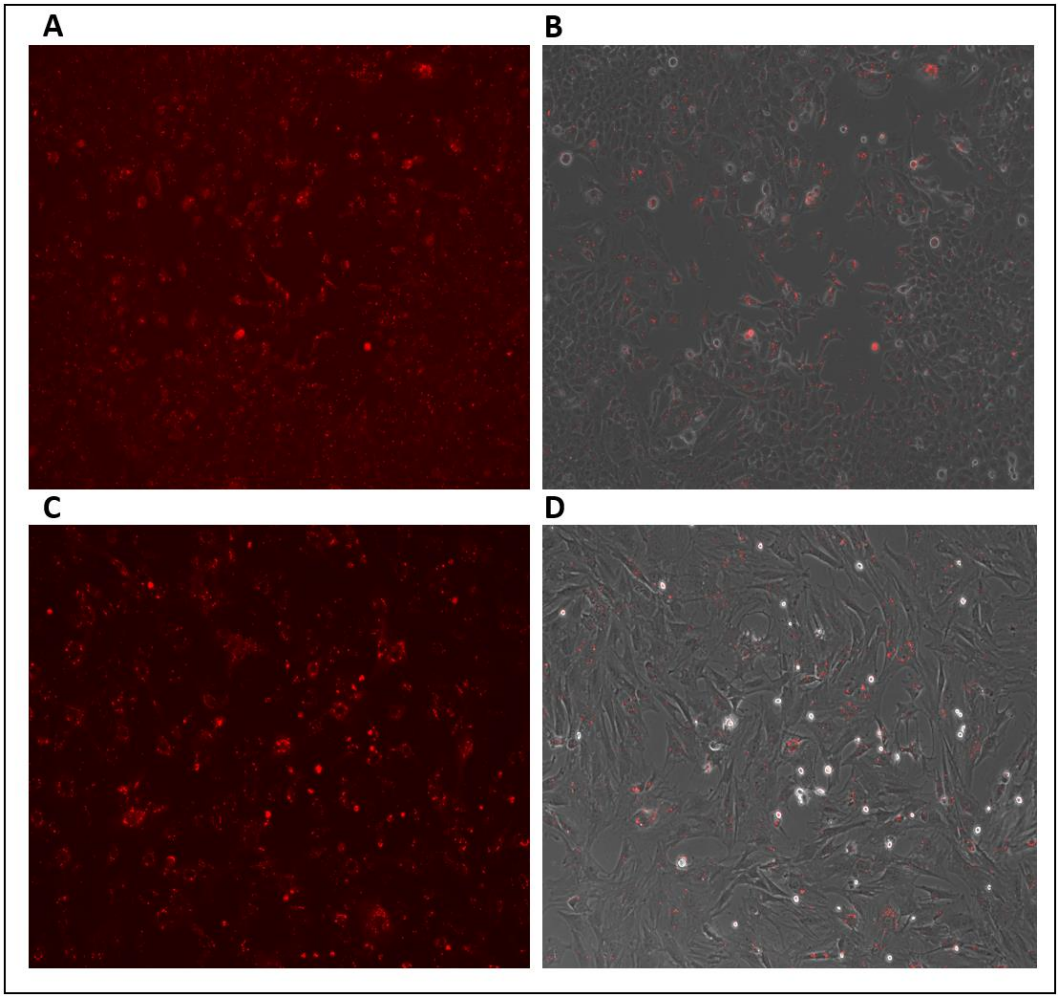

Figure 5: 40x magnification images from EVOS microscope (A) Image of UMR-106 cells with 10nM fluorescent-labelled transfection control (B) Phase-contrast and fluorescence overlay images of UMR-

106 cells (C) Image of BMSCs with 10nM fluorescent-labelled transfection control (D) Phase-Contrast and fluorescence overlay images of BMSCs. Red is an indicator of siRNA transfection

2.2 Silencing of GLUT-1, GLUT-3, and GLUT-4 in UMR-106 cells

To check how effectively the combination of three siRNA constructs targeted for the different sites of the same transcript have silenced the gene expression, the mRNA expression of GLUT-1, -3, and -4 was analysed by qPCR. Results from qPCR showed a significant reduction in GLUTs mRNA expression in both UMR-106 osteosarcoma cell line and BMSCs.

Figure 6 (A) demonstrates that when GLUT-1 is silenced in UMR-106 osteosarcoma cell line with 10 nM concentration of siRNA then mRNA expression is 85% downregulated compared with scramble construct ($P < 0.0031$). The effect on the gene expression of GLUT-3 remained unchanged when GLUT-1 is silenced whereas, GLUT-4 gene expression was moderately upregulated ($P < 0.0221$).

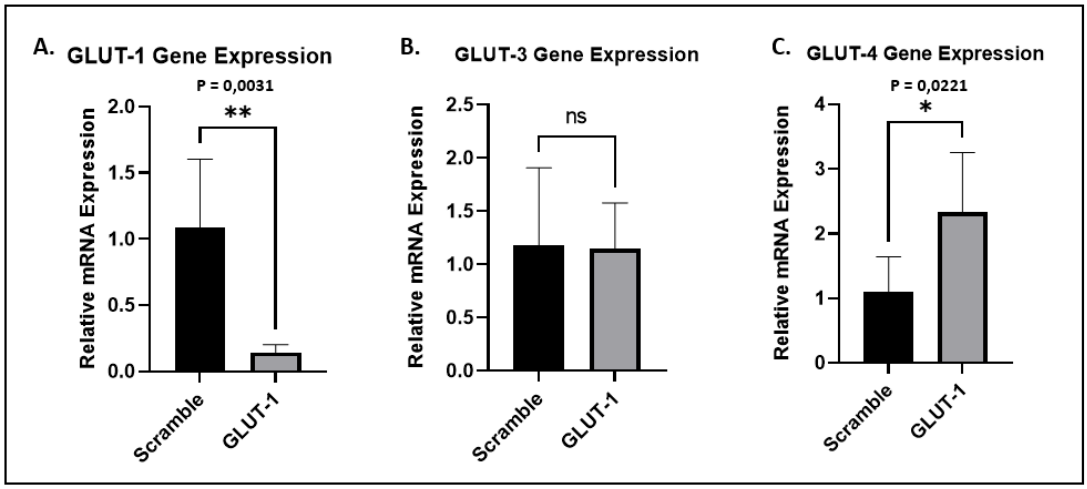

Figure 6: Silencing of GLUT-1 using 10 nM siRNA in UMR-106 cell line after 48 hours transfection (A) GLUT-1 gene expression (B) GLUT-3 gene expression (C) GLUT-4 gene expression

Similarly, as seen in Figure 7 (A) GLUT-3 gene expression was 97% downregulated when compared with control ($P<0.0079$). Whereas gene expression of GLUT-1 and GLUT-4 were not significantly changed when GLUT-3 was silenced with 10 nM concentration of the siRNA.

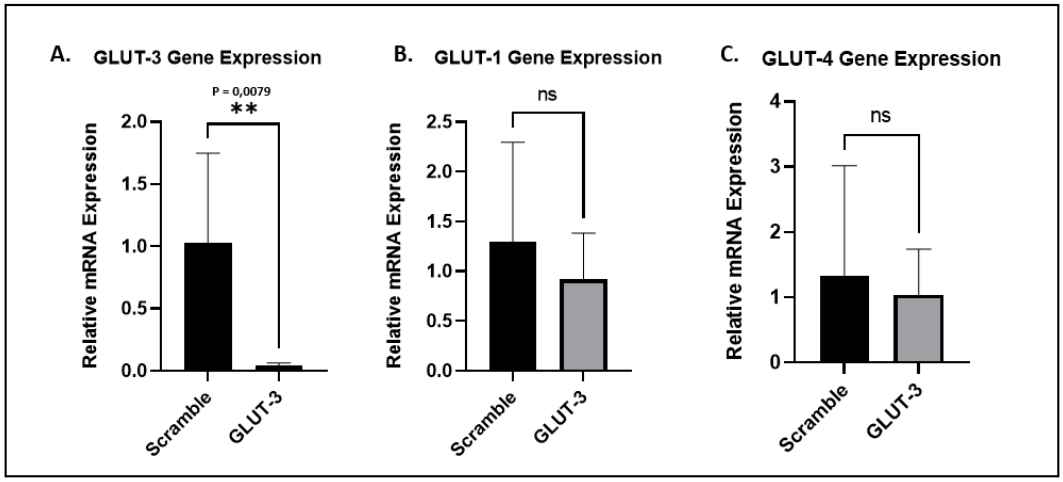

Figure 7: Silencing of GLUT-3 using 10 nM siRNA in UMR-106 cell line after 48 hours transfection (A) GLUT-3 gene expression (B) GLUT-1 gene expression (C) GLUT-4 gene expression

Figure 8 (A) demonstrates that GLUT-4 gene expression in UMR-106 osteosarcoma cell line was 94% downregulated ($P<0.0004$) which shows a significant downregulation of the gene expression when compared with control. GLUT-4 silencing did not affect the expression of GLUT-1 or GLUT-3 ($P > 0.05$) in figure 8 (B) and (C).

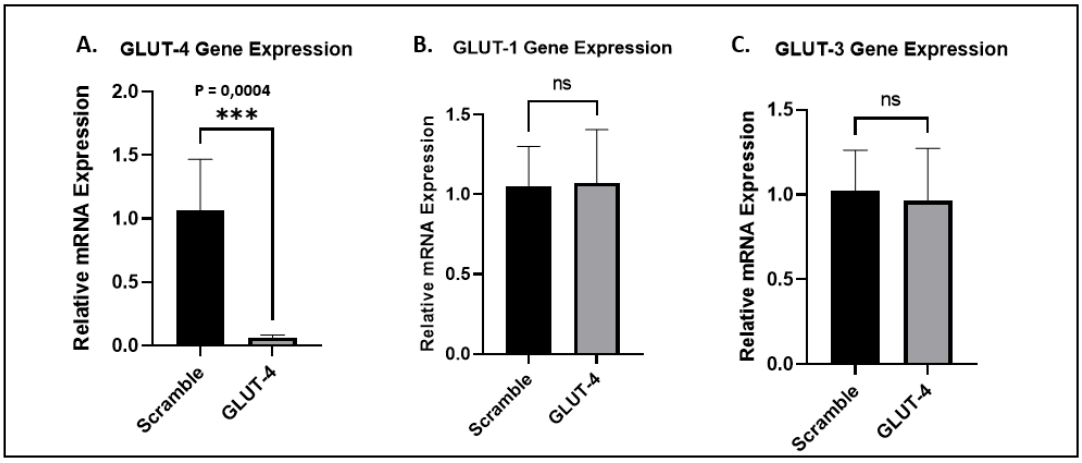

Figure 8: Silencing of GLUT-4 using 10 nM siRNA in UMR-106 cell line after 48 hours transfection (A) GLUT-4 gene expression (B) GLUT-1 gene expression (C) GLUT-3 gene expression.

2.3 Silencing of GLUT-3 in rat bone mesenchymal stromal cells

GLUT-3 gene expression in rat BMSCs after 48 hours of gene silencing was not statistically significant. As this experiment was performed with only two samples, hence we need to repeat our experiment for 48-hour time point but initially our results represent in Figure 9 that GLUT-3 gene expression is tended to be downregulated when it has been silenced with the 10 nM siRNA treatment.

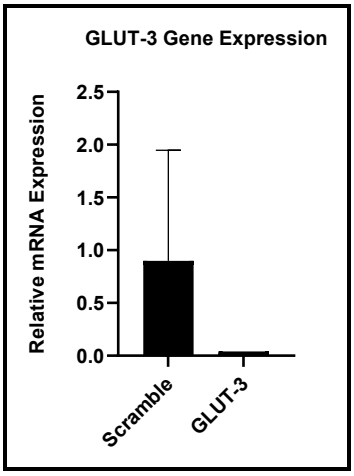

Figure 9: Silencing of GLUT-3 using 10 nM siRNA in BMSCs

2.4 Detection of GLUT-1, -3 and -4 proteins using Immunofluorescence

Initially we confirmed the expression of GLUTs at the sub-cellular level in UMR-106 with immunohistochemical analysis of GLUT-1, -3, and -4 using fluorescence Zeiss imager microscope. Also, we have checked the proteins expression of GLUT-1, 3 and 4 when they have been silenced with the siRNA at 48-hour time point as shown in Figure 10, 11 and 12. The positive control without siRNA treatment, represents GLUTs proteins at subcellular level whereas, the negative control, without the primary antibody for GLUT-1 was used to confirm non-specific signal.

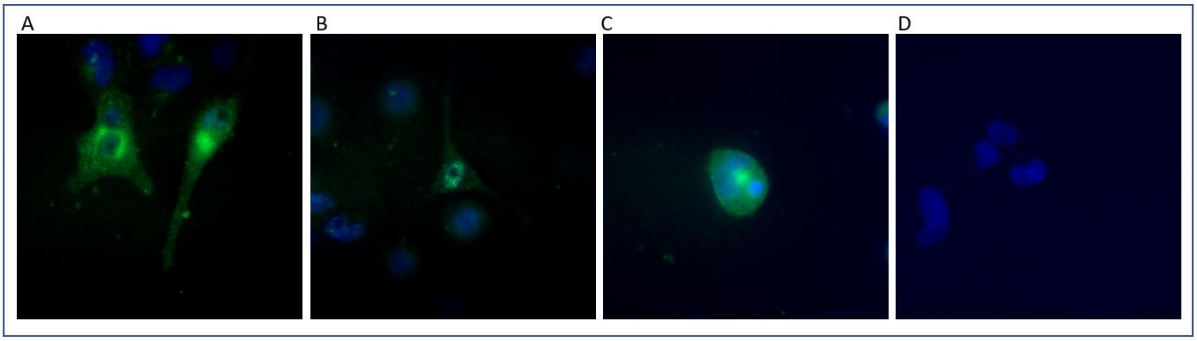

Figure 10: Fluorescence microscopic images with 40x magnification showing GLUT-1 protein localization at sub-cellular level after 48 hours of 10nM siRNA treatment (A) Scramble siRNA (B) GLUT-1 siRNA silencing (C) Positive control (without treatment) (D) Negative control (without primary antibody)

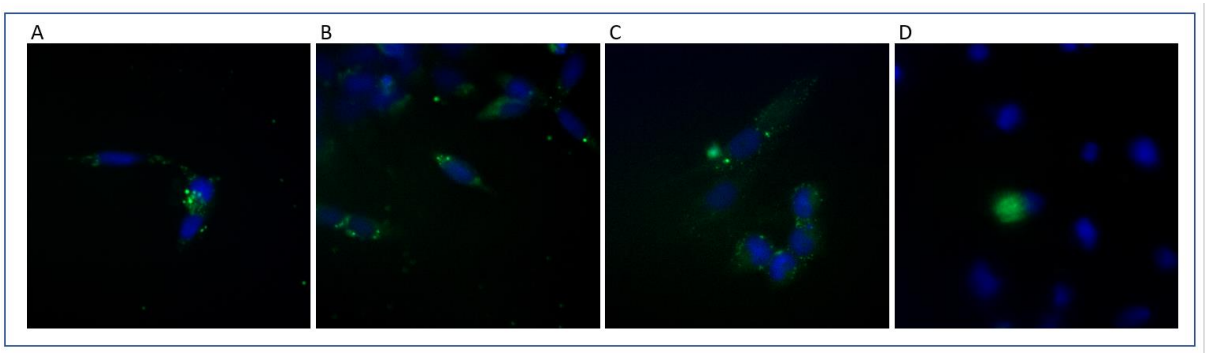

Figure 11: Fluorescence microscopic images with 40x magnification showing GLUT-3 protein localization at sub-cellular level after 48 hours of 10nM siRNA treatment (A) Scramble siRNA (B) GLUT-3 siRNA silencing (C) Positive control (without treatment) (D) Negative control (without primary antibody)

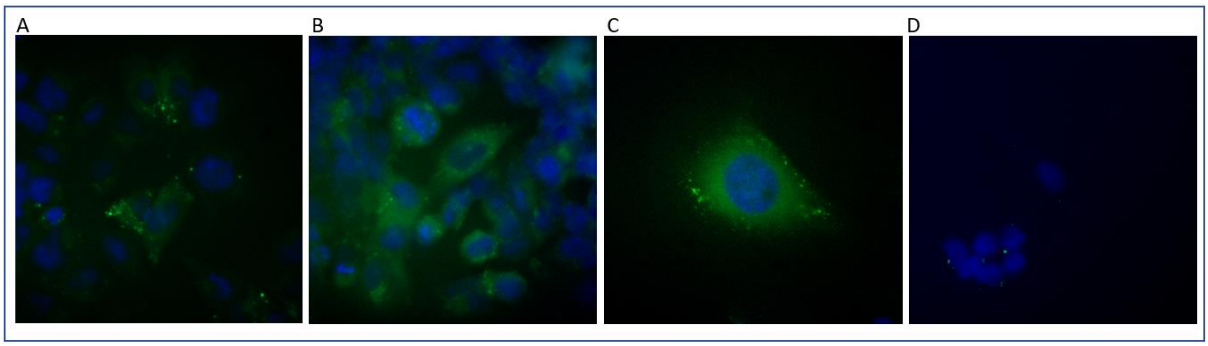

Figure 12: Fluorescence microscopic images with 40x magnification showing GLUT-4 protein localization at sub-cellular level after 48 hours of 10nM siRNA treatment (A) Scramble siRNA (B) GLUT-4 siRNA silencing (C) Positive control (without treatment) (D) Negative control (without primary antibody)

The silencing effect of GLUT gene expression by siRNAs was not efficient enough to reduce the protein level of respective GLUT proteins 48 hours after transfection.

2.5 Viability of UMR-106 cells after transfection

AlamarBlue™ assay was performed to check the viability of cells. Figure 13 demonstrates that when cells were treated with the lipofectamine as a transfection reagent as well as with the three constructs of the 10 nM siRNA individually for each GLUT-1, -3 and -4, the cells remain viable when compared to untreated cells. The siRNA treatment alone for each GLUT did not significantly affect the viability of UMR-106 cells after 48 hours. In contrast, combination of siRNAs for all three GLUTs at the same time reduced the viability of osteoblastic cells. To confirm these results, we need to further repeat these experiments to verify our results.

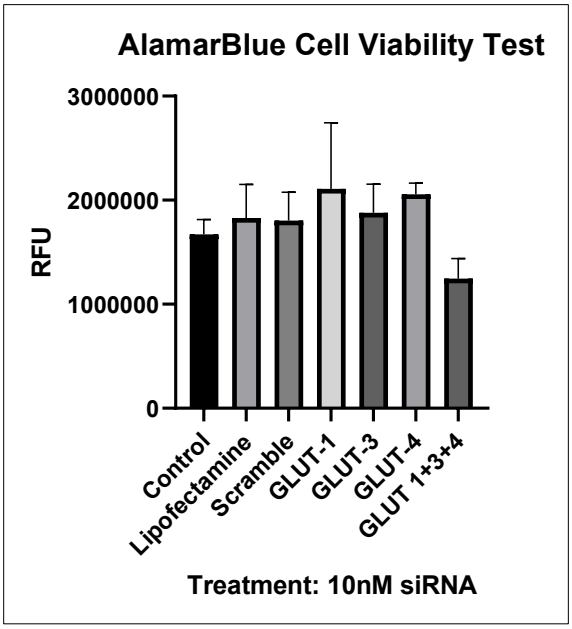

Figure 13: Viability of cells by AlamarBlue™ assay.

2.6 Gel Electrophoresis and qPCR for other GLUTs

Primers for GLUT-5, -8, -9, -10 and -12 were designed at www.ncbi.nlm.nih.gov/tools/primer-blast website and purchased from IDT DNA as mentioned in methodology. While primers for GLUT-6 and -7 require further optimization and GLUT-11 is not included in our experiments as it is not expressed in mice or rats (Scheepers et al., 2005). Efficiency of primer pairs was checked, and we also optimized PCR conditions for each GLUT primer by testing for optimal annealing temperatures between 57 to 60 degrees

C. Final Tm for each GLUT primer is mentioned in table 2. Figure 14 demonstrates the efficiency of our selected GLUT primers, where only GLUT-10 primer pair has efficiency within recommended range from 90% to 110% ensuring quantitative amplification. While other GLUT primer pairs had efficiency >110% due to which they need further optimization or redesign of new primers is required.

Table 2: Positive control tissues and Tm for qPCR for glucose transporter primers

Targeted genes	**Positive control tissue**	**Final Tm**
GLUT-5	Liver	60
GLUT-8	Brain	57
GLUT-9	Liver	57
GLUT-10	Heart	58
GLUT-12	Muscle	57

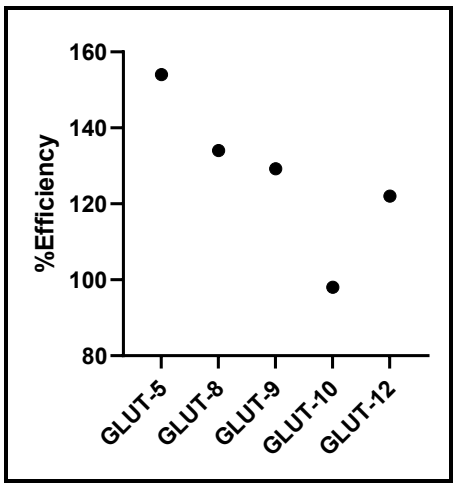

Figure 14: Efficiency (%) of primers for glucose transporters

RT-qPCR was performed to detect the gene expression of other GLUTs and then agarose gel electrophoresis was used to verify the specificity of the amplification. We have checked the expression of GLUT-5, -8, -9, -10 and -12 not only in positive control tissues but also in UMR-106 cell line, BMSCs and cells differentiated to osteoblasts for 8 days (OB). Figure 15 represents original amplification curves from RT-qPCR representing the expression of GLUTs-5, -8, -9, -10 and -12 in all the samples evaluated,

although with different Ct values for different tissues. Gel electrophoresis was performed from endpoint samples (amplified for 40 cycles) to confirm the size of the amplicon.

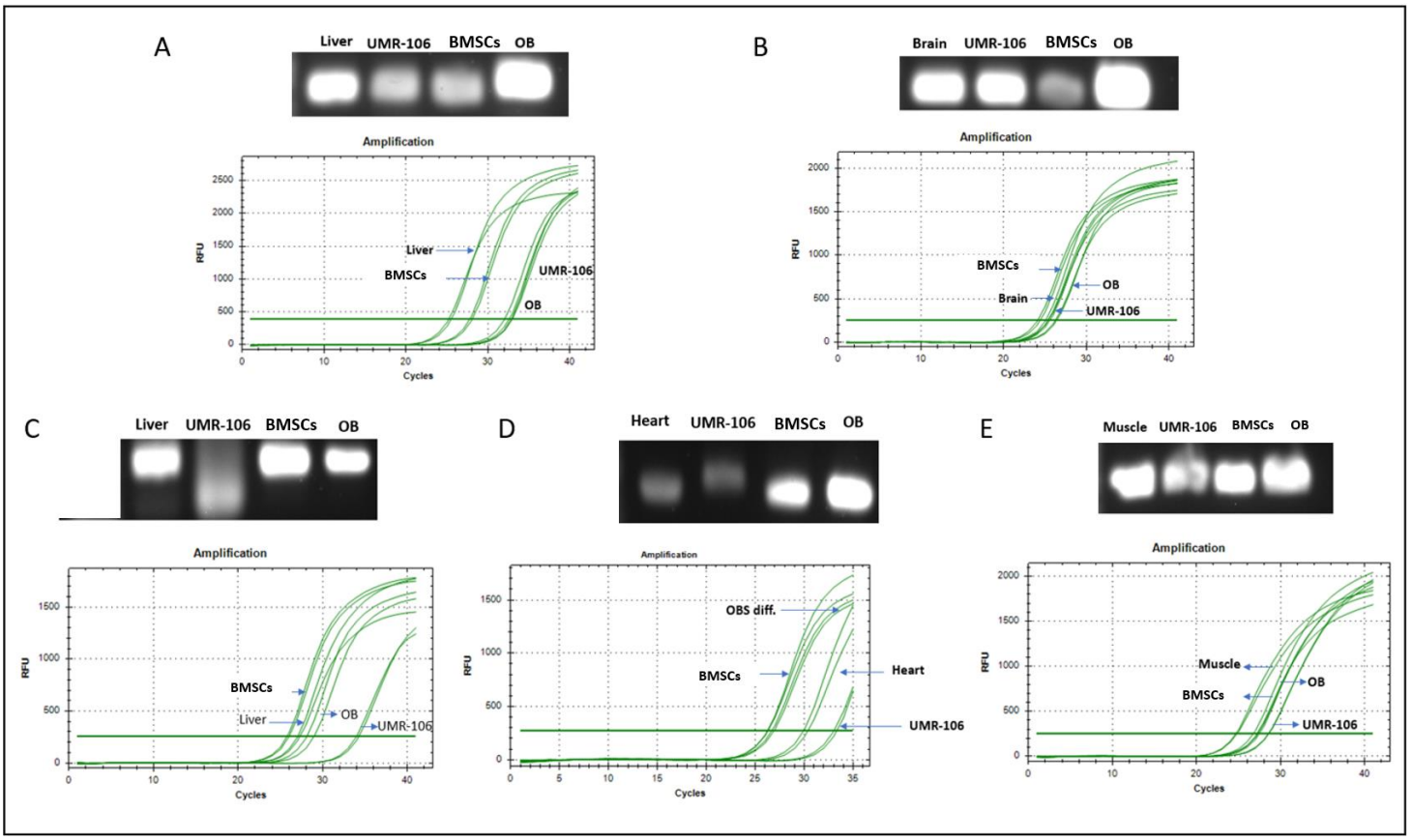

Figure 15: Glucose transporters gene expression in positive tissues, UMR-106 cell line, BMSCs and OB cells (A) GLUT-5 gene expression (B) GLUT-8 gene expression (C) GLUT-9 gene expression (D) GLUT-10 gene expression (E) GLUT-12 gene expression

3. Discussion

The role of various GLUTs in osteoblastic differentiation and maturation is poorly understood. Among glucose transporters GLUT-1, -3 and -4 are known as high affinity transporters and are found in many tissues with a high metabolic activity, such as liver, brain, and muscles (Mobasheri, 2012). It has been reported that GLUT-1 and GLUT-3 are expressed in rat osteosarcoma cell lines UMR-106-01 (Thomas et al., 1996). Based on the GLUT-1 knockout mouse model, it was discovered that GLUT-1 is the most important transporter in monolayer cultures of primary osteoblasts (Lee et al., 2017). Wei et al also studied, that osteoblast cells utilize glucose for their function and GLUT-1 facilitated glucose uptake is a critical signal that begins the initial commitment of osteoblast by regulating the stability of Runx2 (Wei et al., 2015).

The main objective of this study was to determine the role of GLUTs in osteoblastic cells. Currently, we have been able to establish a methodology for silencing of GLUTs which may help us to find the role of GLUTs in primary osteoblastic cells. We used qPCR to detect the mRNA expression of GLUTs and siRNA technology has been used to get an insight of GLUT-1, -3, and -4 importance. We used lipofectamine and siTran 2.0 as delivery method of siRNA into the cells. Lipofectamine is a RNAi-specific liposomal transfection reagent that has positive charge and makes a complex with nucleic acids negative charge. While siTran 2.0 is a non-liposomal siRNA transfection reagent which was purchased from Origene company, and its composition is confidential therefore its methodology is unknown. For UMR-106 cell line, lipofectamine was used as a transfection reagent. While for BMSCs, our experiments showed that lipofectamine was toxic to the cells whereas siTran 2.0 worked efficiently as a transfection reagent.

We selected rat as the model organism in our research as rat physiology resembles human physiology more as compared to murine physiology, particularly when it comes to osteoblast biology. Also, rat has a longer body size allowing more cells to be obtained per animal for a cell culture experiment as compared to mice (Iannaccone and Jacob, 2009). Due to rapid growth of cell lines compared to primary osteoblasts, we started our experiments with rat osteosarcoma cell line UMR-106 to optimize the methodology and continued further optimizations in rat-derived BMSCs.

The siRNA technique is an efficient and specific method to achieve a successful silencing of specific mRNAs in the target tissue or cell. The advantage of this technique precedes the disadvantages as it can be used for various in vitro and in vivo treatments, where it can target any gene with great efficiency and

specificity. Due to selective permeability of a cell membrane, the siRNA molecules have some disadvantages that they possess unfavourable physicochemical properties, such as a negative charge, large molecular size, or weight but these issues can be solved to some extent by nanocarriers (Wang et al., 2010). There are difficulties with siRNA technology when used in bone cells as siRNA systemic delivery to bone is not efficient since it is not a highly perfused tissue (Liu, 2016). On the contrary, siRNA has been delivered directly to the bone via local delivery and siRNA delivery method can be used for different bone sites, including wrist, femur, and vertebral spine. The delivery of siRNA within a localized area has less barriers than delivery from a systemic area (Wang et al., 2010).

Our experiments were initiated by the optimization of siRNA concentration to get highest transfection efficiency with optimal/minimal siRNA concentration. We transfected both UMR-106 cell line and primary BMSCs using concentrations of 1 nM, 2.5 nM, 5 nM and 10 nM siRNA. Both UMR-106 cell line and BMSCs had high transfection efficiencies with 10 nM of fluorescently labelled siRNA.

In our experiments, we used combination of three different siRNAs that all silenced either GLUT-1, GLUT-3, or GLUT-4. The binding of three different constructs of siRNA (constructs A/B/C) were specific at three different sites of each target (GLUT-1, -3 or -4). While 10 nM of each GLUTs siRNA showed not only low cytotoxicity and high transfection efficiency but also it is appropriate for >90% gene silencing in both UMR-106 cell line and BMSCs. The 10nM concentration silenced 85% of GLUT-1, 97% of GLUT-3, and 94% of GLUT-4 in UMR-106 respectively. The 27-mer siRNA constructs A/B/C resulted in an efficient gene silencing at RNA level in both UMR-106 cell line as well as in BMSCs based on qPCR. Hence, the conclusion was made that the siRNA constructs A/B/C from OriGene company has efficiently worked by targeting a specific gene and silenced GLUTs in both UMR-106 cells and in BMSCs.

As osteoblastic cells need energy for bone formation hence it is important to consider that when one of the GLUTs is silenced then there is a possibility that other GLUTs are upregulated to compensate the energy mechanism. Therefore, in addition to class-I GLUTs, we also examined the mRNA expression of other GLUTs 5, -12 in both UMR-106 cell line and rat BMSCs. GLUT-11 was not included in the study as it has been suggested that GLUT-11 is not expressed in mice and rats (Scheepers et al., 2005). Primers for GLUTs 5-10 and -12 were designed and with RT-qPCR the expression of GLUT-5, -6, -7, -8, -9, -10 and -12 in positive control tissues were detected. GLUT-6 and GLUT-7 PCR still require further optimization. The results obtained from RT-qPCR and gel electrophoresis shows the presence of GLUT-

5, -8, -9, -10 and -12 in UMR.106 rat osteosarcoma cell line, undifferentiated BMSCs and mature osteoblasts. These initial findings suggest that there might be other GLUTs than classical glucose transporters that contribute as an energy source to osteoblastic cells. At present, we need to further optimize our protocols and repeat these experiments to confirm these outcomes.

We established that siRNA silencing was effective at RNA level, therefore experiments were proceeded to protein levels. Cells were treated with siRNA and then strained with antibodies detecting GLUTs to determine whether there is a decrease in protein levels. We did not observe downregulation of GLUT protein in cells treated with siRNA constructs using immunofluorescence. Therefore, silencing of GLUTs with siRNA for 48 hours was not enough to achieve efficient silencing of GLUT proteins.

Our initial findings suggests that we may need to consider longer siRNA silencing period than 48 hours used in this study to achieve silencing of GLUT proteins. For UMR-106 cells, we used lipofectamine as a transfection reagent in a 6-well plate, whereas for immunofluorescence studies siTRAN 2.0 transfection reagent was used. It was observed that lipofectamine was more toxic to cells as compared to siTRAN 2.0 as transfection reagent in 24-well plate. In future, we need to repeat these experiments to further validate our findings.

One of the aims of this project was to silence GLUTs either individually or in combination and find out that which could be the most important for the viability of the cell. Also, we assessed the effect of lipofectamine transfection reagent on cells viability. At present, we have been only able to perform initial experiments with UMR-106 cells to check their viability after siRNA transfection and GLUT silencing. Our results suggests that lipofectamine as a transfection reagent does not reduce viability. Moreover, when GLUTs in UMR-106 cells were silenced in combination of siRNA of each GLUT-1, -3, and -4 then cells viability was reduced as compared to when they have been treated individually with each specific GLUT siRNA.

In the future, cell proliferation analysis will be done to confirm the reduced viability in triple silenced cells, for instance by assessing confluence with IncuCyte® Live Cell Imaging. The uptake of glucose in silenced cells will also be analysed by uptake of fluorescently labelled glucose analogue (2-NBDG Glucose Uptake Kit).

There are some limitations related to this project such as for immunofluorescence, when GLUT-1, -3 and -4 were silenced with siRNA for 48-hours the amount of GLUT proteins was not reduced even by the

elimination of their target mRNA that encoded them. One of the reasons for this issue could be because of GLUT proteins half-life as they already exist in the cells even before siRNA silencing as proteins disappearance relies on their half-life. Also, it was not known if silencing is efficient enough at protein level. The transfection of siRNA was done with transfection reagents due to which the silencing of GLUT genes was transient as seen in immunofluorescence. Therefore, we need to consider longer time for silencing of GLUT proteins at protein level. Another option would be to silence GLUTs with lentiviral transfection of siRNA to get more stable and longer-term silencing. Besides, the primary cells exhibit heterogenous nature, are more expensive as they require additional nutrients or growth factors as compared to cancerous cell lines. Therefore, they function differently from one culture to another. Another limitation was that we performed our experiments using rodent as a model. To further validate our methods and findings, this study can be performed with silencing GLUTs in human cells.

Previously, it has been observed that Runx2 is not only required for osteoblastic differentiation and mineralization but also it is an important regulator for uptake of glucose in osteoblast and for GLUT-1 expression (Wei et al., 2015). It will be interesting to study the effect of GLUTs silencing on the expression of transcriptional factors such as Runx2 and on bone proteins like ALP and OCN. GLUT-4 activation is dependent on the levels of insulin therefore, it may be interesting to evaluate the expression of insulin receptor when GLUT-4 has been silenced with siRNA.

The cancerous cells consume large amount of glucose as a source of energy, and it has been studied that GLUT-1 and GLUT-3 are highly expressed in osteosarcoma cells (Cifuentes et al., 2011). Previously, RNAi has been used to downregulate GLUT-1 expression in osteosarcoma cell line MG63 *in vitro* (Fan et al., 2010). The expression of GLUT-1 was confirmed at RNA level in MG63 cells by using RT-qPCR and at protein levels by western blotting. After confirmation, GLUT-1 expression was silenced with RNAi. When the downregulation of GLUT-1 occurred, the uptake of glucose in the cells was inhibited and proliferation of MG63 cells was reduced *in vitro*. This suggests that inhibition of GLUT-1 could be a successful approach for the therapy of osteosarcoma patients (Fan et al., 2010). The siRNA silencing of GLUTs in UMR-106 rat osteosarcoma cell line can be further investigated and in future it may help to develop therapeutic strategies for the treatment of osteosarcoma.

In diabetes, the function of osteoblast is affected leading to fragility of bones and fractures. Additionally, hyperglycaemia affects not only osteoblast's function but also their proliferation and viability (Jiao et al., 2015). Nutritional factors for instance glucose are also necessary for the maintenance and remodelling

of bone. With understanding the energy metabolism of osteoblast and the functions of GLUTs, we can identify new therapy targets for new drugs.

Relatively little is known on bone cell bioenergetics, compared to other tissue. Our research project has provided knowledge on the role of different GLUTs in osteoblasts and their precursors BMSCs. By silencing of each GLUT-1, -3 and -4 individually and in combination with siRNA, we gained an insight into the importance of each GLUT in osteoblast energy metabolism and homeostasis.

We have also established a method for silencing of GLUTs in primary osteoblasts and elucidate the role of each GLUT in osteoblast energy utilization and metabolism.

To summarize, the constructs of siRNA in combination and individually have worked successfully as we have achieved >85% downregulation of GLUTs in both UMR-106 cell lines and in BMSCs. Pre-liminary results also suggest expression of other GLUTs in both osteosarcoma cell line and in BMSCs. our findings have raised further questions related to osteoblast metabolic requirements. Furthermore, this research has assisted us to understand the contribution of bone formation in whole body glucose utilization. For future perspective of drug development and discovery, siRNA technology can be used efficiently for the delivery of a particular molecule to a specific target. We can develop siRNA techniques that can help us to find cures for bone related diseases.

4. Materials and Methods

4.1 Cell line UMR-106 and Cell Culture

Cell line UMR-106 (ATCC® CRL-1661™), a clonal derivative of rat osteosarcoma osteoblast-like cell, receptors for PTH and 1-25(OH)2D3 was obtained from the ATCC (American Type Culture Collection, Manassa, VA, USA) and was maintained in the basal medium of Dulbecco's Modified Eagle's Medium (DMEM). The growth medium was supplemented with 10% fetal bovine serum (Gibco, EU), 1% GlutaMAX™ (Gibco), and 1% Penicillin-Streptomycin (Gibco).

4.2 Rat bone marrow stromal cells

Isolation of bone marrow stromal cells (BMSCs) was done using femur and tibia of a 4-week-old Sprague Dawley female rat and bone marrow was flushed with 22 G needle. Bone marrow cells were cultured in αMEM medium (Gibco, USA) along with 15% fetal bovine serum, 10 mM HEPES (Gibco), 2 mM GlutaMAX™ (Gibco), 1% Penicillin Streptomycin (Gibco) and 10^{-8} M dexamethasone (Sigma). Medium was changed after two days, and cells were then allowed to grow for five days in an incubator and used for transfection experiments. Primary cells were freshly used after the isolation without any long-term subculturing.

4.3 siRNA and transfection reagents

The siRNA constructs (OriGene) include gene specific 27mer siRNA duplexes, three constructs for each GLUT. Universal scrambles negative control siRNA duplex was used as a control. The siRNA are a combination of three different constructs A, B and C for each specific glucose transporter, and it binds at three different sites of GLUT-1 (SR503164A/B/C), GLUT-3 (SR502308A/B/C) and GLUT-4 (SR515187A/B/C). Figure 16 shows the binding of three different constructs of siRNA A, B and C for each specific Glucose transporter and it binds at three different sites of GLUT-1, GLUT.3 and GLUT-4. The sequence of GLUT siRNAs was as followed:

- **GLUT-1 siRNA:**
  - SR503164A- GCUAGAUGAGACCUCUUCCAAACTG
  - SR503164B- GUAACUUUACCUAAGCAGAUAUAAA
  - SR503164C- GGUUGUCUAUUAAAUACAGACACTA

- **GLUT-3 siRNA:**
  - SR502308A- AACUCCAUGCUUCUAGUCAACCUGA
  - SR502308B- GAGACAAUCAUUAAGGACUUUCUTA
  - SR502308C- ACGAUUUCUCUGUUACUGAAGGATG

- **GLUT-4 siRNA:**
  - SR515187A – AUUGCUUCUGGCUAUCACAGUACTC
  - SR515187B – GUGAUUGAACAGAGCUACAAUGCAA
  - SR515187C – CAGCUCUAGAAUACUUCUGUUCCCT

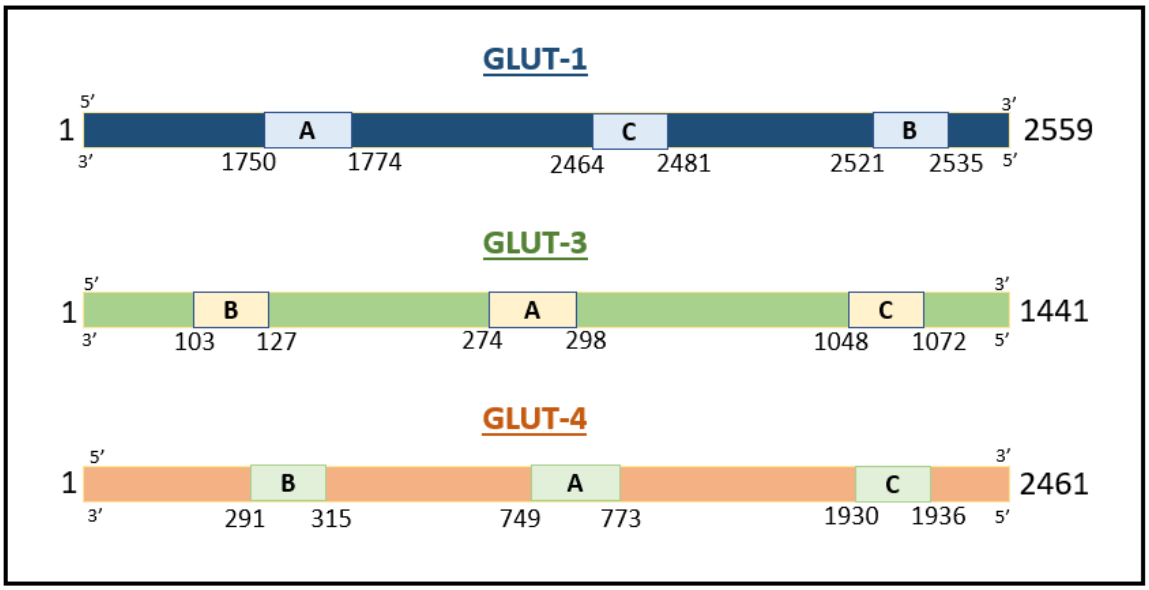

Figure 16: Binding of three different siRNA constructs A/B/C on three different locations of GLUT-1, 3 and 4.

Silencing of GLUT-1, GLUT-3 and GLUT-4 was done by siRNA and transfection reagents were used in this experimental design. For UMR-106 cells, Lipofectamine® RNAiMAX (Thermo Fisher Scientific) was used as a transfection reagent that aids the delivery of 10nM concentration of siRNA into the cells

by endocytosis. Whereas, for primary cells, siTran 2.0 (OriGene) was used as a transfection reagent. To check transfection efficiency of siRNA, 10nM of Trilencer-27 Fluorescent-labelled transfection control siRNA duplex was also used to monitor transfection efficiency with EVOS Auto FL live fluorescence microscope (Thermo Fisher Scientific).

4.4 Methodology for UMR-106 rat osteosarcoma cells

UMR-106 cells were cultured on 75 square centimetre culture flask with DMEM supplemented with 10% iFBS along with the antibiotics and cells were grown to 70-80% confluency in 5% CO_2 atmosphere at 37°C. After that, cells were washed with 1x Phosphate Buffered Saline (PBS, Gibco) and then dissociated from the surface with 0.02% EDTA-trypsin (Thermo) and collected by centrifugation (800 rpm for 10 minutes). The cells were seeded (50,000 cells per well) in a 12-well culture plate (CytoOne®) with a 3.8 square centimetre area per well for each experiment and allowed to grow to 60-80% confluency before siRNA transfection.

The siRNA transfection was done by preparing a mixture of lipofectamine (2 ul) with Opti-MEM (50 ul) (Gibco) and Opti-MEM with 10nM siRNA of each A, B, C and then mixed both mixtures with each other and incubated for 10 minutes. Meanwhile, changed medium of wells from 12-well plate and added 100uL of siRNA mixture drop-wise into each well and kept for incubation at 37°C. Growth medium was changed after 24 hours, and sample for RNA isolation was collected after 48 hours of transfection.

4.5 Methodology for bone marrow stromal cells

BMSCs were cultured for five days in a 75 square centimetre culture flask and medium was changed after 48 hours. After 5 days, when MSCs were around 80% confluent then cells were washed with PBS and collected with 0.05% EDTA trypsin (Gibco). Centrifugation was done for 8 minutes at 1000 rpm and pellet was resuspended with 5 mL of 15% medium and cells were counted manually under the microscope using haemocytometer.

For each experiment, 20000 cells were seeded on a 6 well plate (CytoOne®) with a 9.6 square centimetre area per well and allowed to grow to 75-80% confluency before siRNA transfection. Medium was replaced from each well of 6-well plate with fresh 15% medium 60 minutes before siRNA transfection

and 1x transfection buffer was prepared by adding siTran 2.0 transfection buffer into dH_2O. All siRNA mixtures were prepared with 1x transfection buffer and then siTran 2.0 was added into it. Incubation was done for 15 minutes at room temperature. 100 ul of the siRNA mixture was added to the cells drop-wise and medium was changed 18 hours post transfection. After 48 hours, samples were collected for cell lysis and RNA isolation.

4.6 Cell lysis sample collection and RNA extraction

Collection of RNA lysis sample and RNA extraction for both UMR-106 and BMSCs was done with NucleoSpin RNA Plus, Mini kit for RNA purification with DNA removal column (Macherey-Nagel) according to manufacturer's instructions.

After 48 hours of siRNA transfection, medium was discarded from the wells and 350 ul of Lysis Buffer (LBP) solution was added to each well and cells were scraped properly and transferred to RNAse free Eppendorf tubes. RNA lysis samples were transferred to NucleoSpin gDNA removal column in a collection tube and centrifugation was done for 30 seconds at 11000xg.

Then 100 ul of Binding Solution (BS) was added to the flowthrough and mixed by pipetting and transferred to the NucleoSpin RNA Plus Column with collection tube. Centrifuged for 15 seconds at 11000xg and discarded flow through and changed collection tube.

200 ul of Wash Buffer (WB1) was added to the column and centrifuged for 15 seconds at 11000xg and discarded flow through with changing of a new collection tube. Later 600 ul of Wash Buffer (WB2) was added to the column and centrifugation was done for 15 seconds at 11000xg. Flow though was discarded. Again 250 ul of Buffer WB2 was added to the column and centrifuged for 2 minutes at 11000xg. RNA was eluted with 30 ul of RNase free water and centrifuged for a minute at 11000xg.

The RNA concentration was quantified with NanoDrop ND-1000 device (NanoDrop Technologies) at the absorbance of 260 nm along with RNA purity that was verified by the absorbance ratio of 260/280.

4.7 Reverse Transcription

1 microgram of total RNA was transcribed reversely by adding required amount of Nuclease free water (Thermo Scientific), 5 uM oligo-dT primer (New England Biolabs), 0.5 mM of dNTP mix (Thermo Scientific) to each total RNA sample in microfuge tube and placed in thermocycler for 5 minutes at 65°C

for denaturation of RNA. Once the denaturation of RNA occurred, master mix was prepared by adding Reverse Transcriptase buffer 1x (Thermo Scientific), 200 U Maxima Reverse Transcriptase (Thermo Scientific) and 20 U RNAse Inhibitor (Promega) and 5.5ul of it was added in each microfuge tube for conversion of mRNA to complementary DNA (cDNA) for 30 minutes at 50°C followed by enzyme inactivation at 85°C for 5 minutes. The reaction samples were then diluted with required amount of Nuclease free water for qPCR.

4.8 Quantitative polymerase chain reaction (qPCR)

qPCR was performed to determine the expression of mRNA of GLUTs in both the UMR-106 cell line and BMSCs. qPCR quantitatively analysed the mRNA expression levels of genes via cDNA transcripts from mRNA. With specific primers, qPCR had amplified and quantified the target sequence. SYBR Green dye (Thermo Fisher Scientific) is DNA binding fluorochrome that was added to PCR reactions to get fluorescence when it bonded with double stranded DNA. Then amount of fluorescence was measured after each PCR cycle using qPCR equipment (Bio-Rad). We have used previously designed primer pairs for rat GLUT-1, GLUT-3, and GLUT-4. Cyclophilin B was used as a reference gene.

For each experiment qPCR was performed by preparing 1:10 cDNA sample dilutions with Nuclease free water. Whereas master mix was prepared by adding required amount of Nuclease free water, 0.5 uM of forward primer, and reverse primer for each specific GLUT (Primer sequences purchased from Oligomer, Finland is provided in Appendix 1 Table 1) and Dynamo HS SYBR Green (Thermo Scientific). 4 ul of cDNA dilution sample was added to the wells of each white PCR strips (Bio-Rad) in duplicate along with 6 ul of master mix and closed with caps firmly and spined for few seconds before running in qPCR machine.

The CFX96 Real-Time system C1000 Thermal cycler (Bio-Rad) was used to carry out PCR reaction in three steps whereas overall 34 reaction cycle were selected. To normalize the data, mRNA expression of Cyclophilin B was used. Threshold cycle (CT) value was collected to observe relative gene expression and ΔΔCT method (Livak and Schmittgen, 2001) was used to quantify the results. For all three GLUTs following qPCR conditions were selected:

1. Denaturation: 95°C for 15 seconds
2. Amplification (34 cycles):

- Denaturation: 94°C for 10 seconds
- Annealing: 58°C for 30 seconds
- Extension: 72°C for 20 seconds

3. Final Extension: 95°C for 5 seconds

4.9 Immunofluorescence

Immunofluorescence was performed in UMR-106 cell line to investigate the GLUT-1, GLUT-3, and GLUT-4 protein expression after they have been silenced with siRNA. 24 well cell culture plate (CytoOne®) with an area of 1.9 square centimetre per well was used for the immunofluorescence. In each bottom of the well, glass coverslips were placed, and cells were seeded on them. After getting around 80% confluency, cells were transfected with GLUT-1, GLUT-3, and GLUT-4 siRNA and siTran 2.0 (OriGene) as a transfection reagent. After 48 hours of transfection, cells were washed once with PBS and fixed with 4% paraformaldehyde solution for 15 minutes at room temperature and permeabilized with 0.05% Triton X-100 for 4 minutes on ice. Blocking of samples was performed with 10% normal goat serum (ab156046) for 1 hour. Thereafter, primary antibody (1 ug/ml in PBS with 0.05% Tween) was added and incubated for overnight at +4° C. List of primary antibodies (all purchased from Abcam) for each specific GLUT is mentioned below in Table 3. After 24 hours of incubation, cells were washed thrice with PBS. For secondary antibody, goat anti-mouse Alexa Fluor 488 (ab150113) and goat anti-rabbit Alexa Fluor 488 (ab150077) were used at 1:1000 dilution. Secondary antibody was incubated for 1 hour in dark. Afterwards, cells were washed with PBS and coverslips were mounted on an object glass with VECTASHEILD® (Vector Laboratories, USA) composed of DAPI for nucleus visualization. Zeiss AxioImager Fluorescence Microscope was used to view the fluorescent samples and ZEN 2 software (Carl Zeiss Microscopy Gmbh, Germany) was used to analyse all the images.

Table 3: Primary antibodies purchased from Abcam for GLUT-1, 3 and 4.

Primary Antibodies (Abcam)	Anti-Glucose Transporter
Mouse monoclonal ab40084	GLUT-1

Rabbit polyclonal ab41525	GLUT-3
Rabbit polyclonal ab654	GLUT-4

4.10 Cell viability assay

Cell viability was assessed with alamarBlue™ cell viability reagent (Invitrogen). The assay was performed with UMR-106 cell line. 7000 cells along with 200 ul of 10% medium were seeded into each 28 wells of a 48 well plate to achieve 50-60% confluency. Number of samples were four for each treatment. For control, cells remained untreated whereas treatment of cells was done with lipofectamine reagent and 10 nM siRNA of scramble GLUT-1, GLUT-3, and GLUT-4. A combination of all three GLUTs (3.3 nM of GLUT-1, GLUT-3, and GLUT-4 siRNA each total 10 nM) was also used. After 24 hours, medium was changed from the each well. AlamarBlue viability assay was performed after 48 hours by making a solution of 10% alamarBlue™ with MEM Alpha (gibco) and added 250 ul of alamarBlue™ solution to each well and incubate for 1 hour. For background, alamarBlue™ solution alone was used. 100 ul of solution from 48 well plate was transferred to 96 well plate without disturbing the cells in duplicate wells. Fluorescence was measured with EnSight™ (PerkinElmer) multimode plate reader at the wavelength of 560/590 nm and data was interpreted by Kaleido™ 3.0 data analysis software.

4.11 Primer's optimization and Gel electrophoresis

Primers for GLUT-5, -8, -9, -10 and -12 were purchased from Integrated DNA technologies. The primer sequences are listed in Table 4. GLUT-6 and GLUT-7 primer pairs need further optimization and redesigning due to which these GLUTs were not analysed. Primers were tested through PCR to verify specificity and efficiency of each primer pair. Amplification of a positive control was performed as a verification. For positive control, total RNA from tissue samples of rat were purchased from ZYAGEN. 1 microgram of RNA was transcribed into cDNA and qPCR was performed according to melting temperature of each GLUT primer. The mRNA expression of each GLUT was also verified with UMR-106 osteosarcoma cells, BMSCs, and osteoblastic differentiated cells (sample used in the experiment was previously prepared in the research group).

Table 4: GLUTs primers sequence

Primers	Forward Sequence	Reverse Sequence
GLUT-5	CTACGTCATAGGACACGCCG	AGGCCCACTTGAATGAACGG
GLUT-8	ACCATCTTTGAGGAGGCCAA	AAACCATGATCACACCCGAC
GLUT-9	ATACATGACACCAGTGGCCC	AGGCCTTGATATACGGCGTG
GLUT-10	AGTAACCTGGCTGGTCCTCA	AAGCCGATGGCACCGATAAG
GLUT-12	CTGTCGAAGGCGAACTATGTG	TAGGGACTGGAGCCCCTTAG

The amplicons of qPCR were subjected to gel electrophoresis by preparing 1.5% agarose gel (BioNordika) in 1x TBE. 1 ul of Midori green direct dye (NipponGenetics) was added to 5 ul of 50bp DNA ladder (New England Biolabs) whereas 0.5 ul of Midori green direct was added to 1 ul 6x gel loading dye (New England Biolabs) along with 3 ul of PCR product of each sample: positive control tissue, UMR-106, BMSCs and osteoblastic differentiated cells. Water was also used as a negative sample for each experiment (data not shown). Amplicon samples were run on the gel at 100V/100mA for 30 minutes and DNA bands on the gel were visualized using Nippon Genetic Imager under UV-LED. For all new primer pairs of GLUTs following qPCR conditions were selected:

1. Denaturation: 95°C for 15 seconds
2. Amplification (40 cycles):
    - Denaturation: 94°C for 10 seconds
    - Annealing: for 30 seconds (For GLUT-8, -9 and -12 57°C, GLUT-10 58°C and GLUT-5 60°C)
    - Extension: 72°C for 20 seconds
3. Final Extension: 95°C for 5 seconds.

5. Statistical Analysis

The results were analysed with Excel and GraphPad Prism. Students T-test was used to evaluate the statistical significance between the groups. P values <0.05 were considered statistically significant.

6. Ethical and confidentiality issues

This study does not include any animal handling and primary cells were obtained from naive Sprague Dawley rats. The animals used under internal permission were already available and controlled by Central Animal Laboratory, University of Turku. The research does not conduct any human related research.

7. Acknowledgement

I want to express my sincere gratitude to my wonderful supervisor Kaisa Ivaska for giving me an opportunity to work in her group and for helping me to understand and explore the world of scientific research. I am deeply grateful for her support, time, guidance, and encouragement.

I am grateful to my second supervisor Milja Arponen for teaching me all the techniques, for all the assistance, patience and having time for discussions. I must acknowledge all the lab members and group members Nicko Widjaja and Niki Jalava for their help and invaluable suggestions.

I wish to thank Ullamari Pesonen and Sanna Soini for their guidance throughout my master's journey. My warmest gratitude to my dear friends Hira, Afra, Nandita and Nesriin for always being there for me.

I am deeply indebted to all my family members especially to my parents Rais and Samina, my sister Anum, my husband Usman and my lovely daughter Onaisah for their invaluable love, kindness, and life-lasting support without which I would not be able to accomplish anything.

Turku, January 2022

Sana Rais

8. List of Abbreviations

ALP-Alkaline phosphatase

BMSCs- Bone marrow stromal cells

cDNA- complementary deoxyribonucleic acid

CT- Cycle Threshold

DMEM- Dulbecco's Modified Eagle Medium

dsRNA- double stranded ribonucleic acid

GLUTs- Glucose transporters

InsR- Insulin Receptor

mRNA- messenger RNA

MSCs- mesenchymal stromal cells

OCN-Osteocalcin

RANKL- Receptor activator of nuclear factor kappa-B ligand

RISC- RNA-induced silencing complex

RNAi- RNA interference

RT-qPCR- Reverse Transcriptase quantitative polymerase chain reaction

RUNX2- Runt-related transcription factor 2

siRNA- short interfering RNA

SLC2A- Solute Carrier 2A

9. References

Ahmad, M., T. Kroll, J. Jakob, A. Rauch, A. Ploubidou, and J. Tuckermann. 2018. Cell-based RNAi screening and high-content analysis in primary calvarian osteoblasts applied to identification of osteoblast differentiation regulators. *Sci Rep*. 8:14045.

Aliabadi, H.M., B. Landry, C. Sun, T. Tang, and H. Uludağ. 2012. Supramolecular assemblies in functional siRNA delivery: Where do we stand? *Biomaterials*. 33:2546–2569.

Augustin, R. 2010. The protein family of glucose transport facilitators: It's not only about glucose after all. *IUBMB Life*. 62:315–333. doi:https://doi.org/10.1002/iub.315.

Barron, C.C., P.J. Bilan, T. Tsakiridis, and E. Tsiani. 2016. Facilitative glucose transporters: Implications for cancer detection, prognosis and treatment. *Metabolism*. 65:124–139.

Bellido, T., L.I. Plotkin, and A. Bruzzaniti. 2014. Bone Cells. *Basic and Applied Bone Biology*. 27–45.

Bentwich, I., A. Avniel, Y. Karov, R. Aharonov, S. Gilad, O. Barad, A. Barzilai, P. Einat, U. Einav, E. Meiri, E. Sharon, Y. Spector, and Z. Bentwich. 2005. Identification of hundreds of conserved and nonconserved human microRNAs. *Nature Genetics*. 37:766–770.

Boskey, A., and R. Coleman. 2010. Aging and Bone. *Journal of Dental Research*. 89:1333–1348.

Boskey, A.L. 2007. Mineralization of Bones and Teeth. *Elements*. 3:385–391.

Boskey, A.L. 2013. Bone composition: relationship to bone fragility and antiosteoporotic drug effects. *BoneKEy Reports*. 2.

Bradshaw, R.A., and E.A. Dennis. 2010. Handbook of Cell Signaling. Elsevier, Gezondheidszorg.

Brewer, P.D., E.N. Habtemichael, I. Romenskaia, C.C. Mastick, and A.C.F. Coster. 2014. Insulin-regulated Glut4 Translocation. *Journal of Biological Chemistry*. 289. doi:10.1074/jbc.M114.555714.

Capulli, M., R. Paone, and N. Rucci. 2014. Osteoblast and osteocyte: Games without frontiers. *Archives of Biochemistry and Biophysics*. 561:3–12.

Caruana, B.T., F.L. Byrne, A.J. Knights, K.G.R. Quinlan, and K.L. Hoehn. 2019. Characterization of Glucose Transporter 6 in Lipopolysaccharide-Induced Bone Marrow–Derived Macrophage Function. *The Journal of Immunology*. 202:1826–1832.

Chen, H., X. Ji, W.C. Lee, Y. Shi, B. Li, D. Abel, D. Jiang, W. Huang, and F. Long. 2019. Increased glycolysis mediates Wnt7b-induced bone formation. *The FASEB Journal*. 33:7810–7821.

Cifuentes, M., M.A. García, P.M. Arrabal, F. Martínez, M.J. Yañez, N. Jara, B. Weil, D. Domínguez, R.A. Medina, and F. Nualart. 2011. Insulin regulates GLUT1-mediated glucose transport in MG-63 human osteosarcoma cells. *Journal of Cellular Physiology*. 226. doi:10.1002/jcp.22668.

Conconi, M.T., M. Tommasini, E. Muratori, and P.P. Parnigotto. 2001. Essential amino acids increase the growth and alkaline phosphatase activity in osteoblasts cultured in vitro. *Il Farmaco*. 56:755–761.

Dawson, P.A., J.C. Mychaleckyj, S.C. Fossey, S. Mihic, A.L. Craddock, and D.W. Bowden. 2001. Sequence and Functional Analysis of GLUT10: A Glucose Transporter in the Type 2 Diabetes-Linked Region of Chromosome 20q12–13.1. *Molecular Genetics and Metabolism*. 74:186–199.

Dwyer, D.S., S.J. Vannucci, and I.A. Simpson. 2002. Expression, regulation, and functional role of glucose transporters (GLUTs) in brain.

Fan, J., J.-Q. Zhou, G.-R. Yu, and D.-D. Lu. 2010. Glucose Transporter Protein 1–Targeted RNA Interference Inhibits Growth and Invasion of the Osteosarcoma Cell Line MG63 *In Vitro*. *Cancer Biotherapy and Radiopharmaceuticals*. 25. doi:10.1089/cbr.2010.0784.

Fattore, A.D. 2012. Bone cells and the mechanisms of bone remodelling. *Frontiers in Bioscience, E*. 4:2302.

Franz-Odendaal, T.A., B.K. Hall, and P.E. Witten. 2005. Buried alive: How osteoblasts become osteocytes. *Developmental Dynamics*. 235:176–190.

Fulzele, K., R.C. Riddle, D.J. DiGirolamo, X. Cao, C. Wan, D. Chen, M.-C. Faugere, S. Aja, M.A. Hussain, J.C. Bruning, and T.L. Clemens. 2010. Insulin Receptor Signaling in Osteoblasts Regulates Postnatal Bone Acquisition and Body Composition. *Cell*. 142. doi:10.1016/j.cell.2010.06.002.

Gaster, M., A. Handberg, A. Scharmann, H.G. Joost, H. Beck-Nielsen, and H.D. Schroder. 2004. GLUT11, but not GLUT8 or GLUT12, is expressed in human skeletal muscle in a fibre type-specific pattern. *Pflgers Archiv European Journal of Physiology*. 448:105–113.

Ghadakzadeh, S., M. Mekhail, A. Aoude, R. Hamdy, and M. Tabrizian. 2016. Small Players Ruling the Hard Game: siRNA in Bone Regeneration. *Journal of Bone and Mineral Research*. 31:475–487.

Hu, R., H. Li, W. Liu, L. Yang, Y.F. Tan, and X.H. Luo. 2010. Targeting miRNAs in osteoblast differentiation and bone formation. *Expert Opinion on Therapeutic Targets*. 14:1109–1120.

Huang, T., R. Liu, X. Fu, D. Yao, M. Yang, Q. Liu, W.W. Lu, C. Wu, and M. Guan. 2016. Aging Reduces an ERRalpha-Directed Mitochondrial Glutaminase Expression Suppressing Glutamine

Anaplerosis and Osteogenic Differentiation of Mesenchymal Stem Cells. *STEM CELLS*. 35:411–424.

Iannaccone, P.M., and H.J. Jacob. 2009. Rats! *Disease Models & Mechanisms*. 2. doi:10.1242/dmm.002733.

Jiao, H., E. Xiao, and D.T. Graves. 2015. Diabetes and Its Effect on Bone and Fracture Healing. *Current Osteoporosis Reports*. 13. doi:10.1007/s11914-015-0286-8.

Jo, S., J. Han, Y.L. Lee, S. Yoon, J. Lee, S.E. Wang, and T.H. Kim. 2018. Regulation of osteoblasts by alkaline phosphatase in ankylosing spondylitis. *International Journal of Rheumatic Diseases*. 22:252–261.

Joost, H.G., and B. Thorens. 2001. The extended GLUT-family of sugar/polyol transport facilitators: nomenclature, sequence characteristics, and potential function of its novel members. *Molecular Membrane Biology*. 18:247–256.

Jurcovicova, J. 2014. Glucose transport in brain – effect of inflammation. *Endocrine Regulations*. 48:1.

Karner, C.M., E. Esen, A.L. Okunade, B.W. Patterson, and F. Long. 2015. Increased glutamine catabolism mediates bone anabolism in response to WNT signaling. *Journal of Clinical Investigation*. 125:551–562.

Karner, C.M., and F. Long. 2018. Glucose metabolism in bone. *Bone*. 115:2–7.

Katsimbri, P. 2017. The biology of normal bone remodelling. *European Journal of Cancer Care*. 26:6.

Kawane, T., X. Qin, Q. Jiang, T. Miyazaki, H. Komori, C.A. Yoshida, V.K.D.S. Matsuura-Kawata, C. Sakane, Y. Matsuo, K. Nagai, T. Maeno, Y. Date, R. Nishimura, and T. Komori. 2018. Runx2 is required for the proliferation of osteoblast progenitors and induces proliferation by regulating Fgfr2 and Fgfr3. *Scientific Reports*. 8:1.

Kenkre, J., and J. Bassett. 2018. The bone remodelling cycle. *Annals of Clinical Biochemistry: International Journal of Laboratory Medicine*. 55:308–327.

Kogianni, G., and B.S. Noble. 2007. The biology of osteocytes. *Current Osteoporosis Reports*. 5:81–86.

Lee, W.C., A.R. Guntur, F. Long, and C.J. Rosen. 2017. Energy Metabolism of the Osteoblast: Implications for Osteoporosis. *Endocrine Reviews*. 38:255–266.

Li, Q., A. Manolescu, M. Ritzel, S. Yao, M. Slugoski, J.D. Young, X.Z. Chen, and C.I. Cheeseman. 2004. Cloning and functional characterization of the human GLUT7 isoform SLC2A7 from the

small intestine. *American Journal of Physiology-Gastrointestinal and Liver Physiology*. 287:G236–G242.

Li, Z., J.L. Frey, G.W. Wong, M.C. Faugere, M.J. Wolfgang, J.K. Kim, R.C. Riddle, and T.L. Clemens. 2016. Glucose Transporter-4 Facilitates Insulin-Stimulated Glucose Uptake in Osteoblasts. *Endocrinology*. 157:4094–4103.

Liu, Q., M. Li, S. Wang, Z. Xiao, Y. Xiong, and G. Wang. 2020. Recent Advances of Osterix Transcription Factor in Osteoblast Differentiation and Bone Formation. *Frontiers in Cell and Developmental Biology*. 8:1575. doi:10.3389/fcell.2020.601224.

Liu, X. 2016. Bone site-specific delivery of siRNA. *In* Journal of Biomedical Research. Published.

Livak, K.J., and T.D. Schmittgen. 2001. Analysis of Relative Gene Expression Data Using Real-Time Quantitative PCR and the 2−ΔΔCT Method. *Methods*. 25. doi:10.1006/meth.2001.1262.

Mallory, A.C., and H. Vaucheret. 2006. Functions of microRNAs and related small RNAs in plants. *Nature Genetics*. 38:S31–S36.

Marks, S.C., and S.N. Popoff. 1988. Bone cell biology: The regulation of development, structure, and function in the skeleton. *American Journal of Anatomy*. 183:1–44.

McAllister, M.S., L. Krizanac-Bengez, F. Macchia, R.J. Naftalin, K.C. Pedley, M.R. Mayberg, M. Marroni, S. Leaman, K.A. Stanness, and D. Janigro. 2001. Mechanisms of glucose transport at the blood–brain barrier: an in vitro study. *Brain Research*. 904:20–30.

McBrayer, S.K., J.C. Cheng, S. Singhal, N.L. Krett, S.T. Rosen, and M. Shanmugam. 2012. Multiple myeloma exhibits novel dependence on GLUT4, GLUT8, and GLUT11: implications for glucose transporter-directed therapy. *Blood*. 119:4686–4697.

McGee-Lawrence, M.E., F.J. Secreto, and F.A. Syed. 2013. Animal Models of Bone Disease-B. *Animal Models for the Study of Human Disease*. 391–417.

Meister, G., and T. Tuschl. 2004. Mechanisms of gene silencing by double-stranded RNA. *Nature*. 431:343–349.

Mobasheri, A. 2012. Glucose: an energy currency and structural precursor in articular cartilage and bone with emerging roles as an extracellular signaling molecule and metabolic regulator. *Frontiers in Endocrinology (Lausanne)*. 3.

Moore, C.B., E.H. Guthrie, M.T. Huang, and D.J. Taxman. 2010. Short hairpin RNA (shRNA): design, delivery, and assessment of gene knockdown. *Methods in molecular biology (Clifton, N.J.)*. 629:141–158.

Mueckler, M., and C. Makepeace. 2008. Transmembrane Segment 6 of the Glut1 Glucose Transporter Is an Outer Helix and Contains Amino Acid Side Chains Essential for Transport Activity. *Journal of Biological Chemistry*. 283:11550–11555.

Mulari, M., J. Vääräniemi, and H.K. Väänänen. 2003. Intracellular membrane trafficking in bone resorbing osteoclasts. *Microscopy Research and Technique*. 61. doi:10.1002/jemt.10371.

Nahian, A., and A.M. AlEssa. 2021. Histology, Osteocytes. StatPearls Publishing.

O'Brien, J., H. Hayder, Y. Zayed, and C. Peng. 2018. Overview of MicroRNA Biogenesis, Mechanisms of Actions, and Circulation. *Front. Endocrinol.* 9:402. doi:10.3389/fendo.2018.00402.

Ono, T., and T. Nakashima. 2018. Recent advances in osteoclast biology. *Histochemistry and Cell Biology*. 149:325–341.

Pino, A.M., M. Miranda, C. Figueroa, J.P. Rodríguez, and C.J. Rosen. 2016. Qualitative Aspects of Bone Marrow Adiposity in Osteoporosis. *Frontiers in Endocrinology*. 7.

Pulford, B., N. Reim, A. Bell, J. Veatch, G. Forster, H. Bender, C. Meyerett, S. Hafeman, B. Michel, T. Johnson, A.C. Wyckoff, G. Miele, C. Julius, J. Kranich, A. Schenkel, S. Dow, and M.D. Zabel. 2010. Liposome-siRNA-Peptide Complexes Cross the Blood-Brain Barrier and Significantly Decrease PrPC on Neuronal Cells and PrPRES in Infected Cell Cultures. *PLoS ONE*. 5:6.

Qiu, Z.Y., Y. Cui, and X.M. Wang. 2019. Natural Bone Tissue and Its Biomimetic. *Mineralized Collagen Bone Graft Substitutes*. 1–22.

Rubert, M., and C. de la Piedra. 2020. Osteocalcin: from marker of bone formation to hormone; and bone, an endocrine organ. *Rev Osteoporos Metab Miner*. 12. doi:10.4321/S1889-836X2020000400007.

Scheepers, A., S. Schmidt, A. Manolescu, C.I. Cheeseman, A. Bell, C. Zahn, H.-G. Joost, and A. Schürmann. 2005. Characterization of the human SLC2A11 (GLUT11) gene: alternative promoter usage, function, expression, and subcellular distribution of three isoforms, and lack of mouse orthologue. *Molecular Membrane Biology*. 22. doi:10.1080/09687860500166143.

Simmons, R.A. 2017. Cell Glucose Transport and Glucose Handling During Fetal and Neonatal Development. *Fetal and Neonatal Physiology*. 3:428–435.

Soysa, N., N. Alles, K. Aoki, and K. Ohya. 2012. Osteoclast formation and differentiation: An overview. *J Med Dent Sci*. 59:65－74.

Tan, G.S., B.G. Garchow, X. Liu, J. Yeung, J.P. Morris, T.L. Cuellar, M.T. McManus, and M. Kiriakidou. 2009. Expanded RNA-binding activities of mammalian Argonaute 2. *Nucleic Acids Research*. 37:7533–7545.

Taxman, D.J., C.B. Moore, E.H. Guthrie, and M.T.H. Huang. 2010. Short Hairpin RNA (shRNA): Design, Delivery, and Assessment of Gene Knockdown. *Methods in Molecular Biology*. 139 – 156.

Thomas, D.M., F. Maher, S.D. Rogers, and J.D. Best. 1996. Expression and Regulation by Insulin of Glut 3 in UMR 106-01, a Clonal Rat Osteosarcoma Cell Line. *Biochemical and Biophysical Research Communications*. 218. doi:10.1006/bbrc.1996.0140.

Thorens, B., and M. Mueckler. 2010. Glucose transporters in the 21st Century. *American Journal of Physiology-Endocrinology and Metabolism*. 298:E141–E145.

Tomari, Y. 2005. Perspective: machines for RNAi. *Genes & Development*. 19:517–529.

Velling, T., J. Risteli, K. Wennerberg, D.F. Mosher, and S. Johansson. 2002. Polymerization of Type I and III Collagens Is Dependent On Fibronectin and Enhanced By Integrins α11β1and α2β1. *Journal of Biological Chemistry*. 277:37377–37381.

Wang, J., Z. Lu, M.G. Wientjes, and J.L.S. Au. 2010. Delivery of siRNA Therapeutics: Barriers and Carriers. *The AAPS Journal*. 12:492–503. doi:10.1208/s12248-010-9210-4.

Wei, J., J. Shimazu, M. Makinistoglu, A. Maurizi, D. Kajimura, H. Zong, T. Takarada, T. Iezaki, J. Pessin, E. Hinoi, and G. Karsenty. 2015. Glucose Uptake and Runx2 Synergize to Orchestrate Osteoblast Differentiation and Bone Formation. *Cell*. 162:1169.

White, M.A., E. Tsouko, C. Lin, K. Rajapakshe, J.M. Spencer, S.R. Wilkenfeld, S.S. Vakili, T.L. Pulliam, D. Awad, F. Nikolos, R.R. Katreddy, B.A. Kaipparettu, A. Sreekumar, X. Zhang, E. Cheung, C. Coarfa, and D.E. Frigo. 2018. GLUT12 promotes prostate cancer cell growth and is regulated by androgens and CaMKK2 signaling. *Endocrine-Related Cancer*. 25:453–469.

Williams, R.S.B., L. Cheng, A.W. Mudge, and A.J. Harwood. 2002. A common mechanism of action for three mood-stabilizing drugs. *Nature*. 417:292–295.

Wu, X., and H.H. Freeze. 2002. GLUT14, a Duplicon of GLUT3, Is Specifically Expressed in Testis as Alternative Splice Forms. *Genomics*. 80:553–557.

Yoder, C.H., J.D. Pasteris, K.N. Worcester, and D. v Schermerhorn. 2011. Structural Water in Carbonated Hydroxylapatite and Fluorapatite: Confirmation by Solid State 2H NMR. *Calcified Tissue International*. 90:60–67.

Zoch, M.L., T.L. Clemens, and R.C. Riddle. 2016. New insights into the biology of osteocalcin. *Bone*. 82. doi:10.1016/j.bone.2015.05.046.

10. Appendix 1

Table 1

	GENE	PRIMER SEQUENCES (5'-3')
GLUT-1	NM_138827.1	F-GCCGCTTCATCATTGGAGTG
		R-GAGTCTAAGCCGAACACCTGG
GLUT-3	NM_017102.2	F-GATCCTTGTGGCTCAGGTCT
		R-ATCTCCGTCGCTTGGTCTTC
GLUT-4	NM_012751.1	F-CGCGGCCTCCTATGAGATAC
		R-ACTCCAAACCCAACACCTGG
CYC-B	NM_022536.1	F-ACCTGTAGGACGAGTGACCT
		R-GCTCTTTCCTCCTGTGCCAT